

Quasielastic ρ^0 electroproduction on the proton at intermediate energy: Role of scalar and pseudoscalar meson exchange

I.T. Obukhovskiy¹, Amand Faessler², D.K. Fedorov¹, Thomas Gutsche²,
Valery E. Lyubovitskij^{2*}, V.G. Neudatchin¹, L.L. Sviridova¹

¹*Institute of Nuclear Physics, Moscow State University,
119991 Moscow, Russia*

²*Institut für Theoretische Physik, Universität Tübingen,
Kepler Center for Astro and Particle Physics,
Auf der Morgenstelle 14, D-72076 Tübingen, Germany*

We present a detailed analysis of ρ^0 electroproduction at intermediate energy for quasi-elastic knock-out kinematics. The approach is based on an effective Lagrangian which generates exchanges of scalar, pseudoscalar, axial-vector and tensor mesons. The specific role of mesons with different values for J^{PC} is analyzed. We show that the π^0 exchange amplitude and its interference terms with $\eta(\eta')$ and f_1 exchanges dominate in the transverse part of the cross section σ_T . The main role plays the $\pi^0 \rightarrow \rho^0$ M1 spin transition when coupling the virtual photons to the nucleon. In contrast, the longitudinal cross section σ_L is generated by a series of scalar meson exchanges. To extract the dominant term more detailed information on the inner structure of scalar mesons is required. It turns out that recent data of the CLAS Collaboration on σ_L and σ_T can be described with reasonable accuracy if one proposes the quarkonium structure for the heavy scalar mesons ($M \gtrsim 1.3$ GeV). On this basis the differential cross sections $d\sigma_L/dt$ and $d\sigma_T/dt$ are calculated and compared with the latest CLAS data.

PACS numbers: 13.40.Gp, 13.60.Le, 14.20.Dh, 25.30.Rw

Keywords: ρ electroproduction, scalar mesons, tensor and axial-vector mesons, strong and electromagnetic form factors

I. INTRODUCTION.

Recent data of the CLAS Collaboration [1, 2] on electroproduction of the ρ^0 meson with separation of longitudinal σ_L and transverse σ_T parts of the cross section open up new possibilities in the study of the production mechanism. Experimental results on σ_L and σ_T obtained at relatively large photon virtualities of $1.5 \lesssim Q^2 \lesssim 4$ GeV²/c² and at invariant energies $W \sim 2 - 3$ GeV (i.e. above the resonance region) supplement the known data of the CLAS Collaboration on ρ^0 photoproduction [3] since they contain new information on the Q^2 -dependence of the cross sections. At large Q^2 some contributions to the cross section are small and in first approximation they can be excluded from the consideration. For example, at $Q^2 \gtrsim 1.5$ GeV²/c² contributions of intermediate baryon states (N , N^* , etc.) to the cross section are sufficiently suppressed in comparison to meson exchange contributions due to form factors encoding finite size effects in the γNN , γNN^* , ρNN and ρNN^* vertices.

An important feature of ρ^0 electroproduction is that different meson exchange mechanisms dominate in the longitudinal and transverse cross sections. This phe-

nomenon allows to consider the contributions of these mesons separately, while the data on only the full cross section $\sigma = \sigma_T + \epsilon \sigma_L$ do not permit such a possibility. For example, data of the JLAB F_π Collaboration on electroproduction of charged pions [4–6] allowed to deduce the charged pion form factor using the dominance of the pion t -pole contribution to the longitudinal part of the differential cross section $d\sigma_L/dt$. Note, that the transverse part $d\sigma_T/dt$ is dominated by the ρ -meson pole, and the JLab data [4–6] on $d\sigma_T/dt$ allow to perform an independent study of the ρ -meson exchange amplitude [7]. It would be impossible to study both phenomena on the basis of the total cross section only.

These new possibilities for a detailed experimental study of the reaction $\gamma_{L,T}^* + p \rightarrow \rho^0 + p$ in quasi-elastic kinematics can be used to gain insight into the structure of the meson cloud of the nucleon and into the quark origin of the electromagnetic properties of neutral mesons. Our present work is devoted to the theoretical study of this reaction in the context of these new possibilities that distinguish recent electroproduction experiments [1, 2] from older ones [8].

In the case of the $\gamma_{L,T}^* + p \rightarrow \rho^0 + p$ reaction until recently there were only integral data (integral characteristics over the t variable – the squared momentum transfer to the proton – see e.g. Ref. [1]) which we have used as a basis for our consideration. Very recently data on the dif-

*On leave of absence from Department of Physics, Tomsk State

Collaboration [2] which allows for a further detailed test of the theory presented here.

The differential cross sections $d\sigma_T/dt$ and $d\sigma_L/dt$ are more informative: for small values of t near the kinematical threshold $t - t_{min} \sim 0$ (i.e. in the region of quasi-elastic meson knockout) the nearby t -channel pole dominates in each of these cross sections, which generates the forward peak of electroproduction in the absorption of either a longitudinal (γ_L^*) or transverse (γ_T^*) virtual photon. In the case of $\gamma_{L,T}^* + p \rightarrow \rho^0 + p$ the pion t -pole contribution dominates in σ_T and t poles of the lightest scalar mesons dominate in σ_L . The dominant t pole gives also a main contribution to the corresponding integrated cross section (σ_T or σ_L), but contributions of heavy-meson exchanges (mesons with masses close to and above 1 GeV) are also important. Sometimes these corrections are quite significant since they interfere with the leading contributions of the light mesons.

Nevertheless, as the first step, the data on σ_L and σ_T [1] for the reaction $\gamma_{L,T}^* + p \rightarrow \rho^0 + p$ can already be used to give an estimate for the dominant contributions. The additional (in comparison to electroproduction of charged mesons) selection rule connected with charge parity (C) conservation in the $\gamma \rightarrow \rho^0$ transition allows this procedure. Latter conservation law reduces the number of exchange diagrams to be considered. Here we also can use the models of vector meson dominance (VMD) and tensor meson dominance (TMD) [9] for an estimate of the vertex constants in the t -channel pole terms [10] using the underlying idea of charge universality.

In the reaction $\gamma_{L,T}^* + p \rightarrow \rho^0 + p$ both the virtual photon and ρ^0 have the same (negative) charge parity, i.e. $J^{PC} = 1^{--}$. Such a reaction cannot be considered as a true quasi-elastic knockout process, since here ρ^0 -meson exchange is forbidden due to C -parity conservation. Therefore, such a “knockout” can proceed due to the conversion of a meson from the nucleon meson cloud into the final ρ^0 meson or due to the $\gamma \rightarrow \rho^0$ transition in a diffraction process. Since pion exchange ($J^{PC} = 0^{-+}$) is allowed here the pion pole must dominate in the region of small $|t|$ (i.e. at small angles in quasi-elastic kinematics). However, the pion contribution only dominates in the transverse part of the cross section σ_T due to the $M1$ spin transition $\pi^0 \rightarrow \rho^0$. At the same time, the pion pole contribution to σ_L is negligibly small even at values of $t \sim t_{min}$ – opposite to the situations of charged meson knockout processes. Pomeron exchange ($C = +$) is allowed but its contribution to σ_L is too small in the region of invariant energies $W \sim 2 - 3$ GeV considered when compared to the summation of the t -pole terms of other low-mass mesons.

For invariant energies W slightly above the baryon resonance region and for high virtualities of the photon ($Q^2 \sim 1.5 - 4$ GeV²/c² in the JLAB experiments) it is sufficient to take into account the exchanges of neutral pseudoscalar mesons and additionally from the three nonets $J^{PC} = J^{++}$ with $J = 0,1,2$ corresponding to the

ble I). Note, that we only consider mesons with positive charge parity (C=+) which give a contribution to the quasi-elastic knockout of ρ^0 supplemented either by spin flip ($M1$ -transitions $^1S_0 \rightarrow ^3S_1$ without changing the spatial P -parity) or deexcitation of the orbital $1P$ state ($E1$ -transitions $^3P_J \rightarrow ^3S_1$ with change of the P -parity). In the first approximation one can neglect the highly excited meson nonets, because the corresponding orbital matrix elements of the transitions $2S \rightarrow 1S$, $2P \rightarrow 1S$, etc. must be suppressed in comparison to the $1S \rightarrow 1S$ and $1P \rightarrow 1S$ contributions.

Starting with energies of $W \sim 5 - 10$ GeV and above the electroproduction cross section is suitably described in the framework of Regge phenomenology, which gives a reasonable description in a wider region of the variable t than the t -pole approximation, – up to the region of hard collisions where partonic degrees of freedom become manifest. Then the most convenient description of the hadronic processes can be done in terms of generalized partonic distributions (see, e.g. [1, 2, 11, 12]).

In a series of works [13–16] the Regge phenomenology has been extended to the description of meson electro- and photoproduction cross sections at lower energies of about $W \sim 2 - 3$ GeV. In this approach meson propagators in the exchanged diagrams are substituted by amplitudes of the corresponding Regge trajectories (R). The Pomeron trajectory (P) contribution is also included in the total sum. Here the coupling constants and form factors of low-energy hadron physics are used for the $\gamma R \rho$ and RNN vertices. For the $\gamma R \rho$ vertex the dominance of vector mesons is used and a corresponding form factor is calculated in terms of the $q\bar{q}$ loop in the Landshoff-Donnachie approach [17]. Since the vertex coupling constants (excluding the πNN coupling) are only known with a low precision an additional free parameter [15, 16] is introduced into the amplitude which is normalized by data on ρ^0 photoproduction.

We should stress that in the energy region of $W \sim 2 - 3$ GeV an equally good description of meson photo- and electroproduction cross sections can also be obtained on the basis of the usual pole approximation – also using phenomenological vertex form factors [7, 10, 18, 19]. An advantage of the pole approximation is that the starting point is set up by effective Lagrangians. Therefore the momentum-spin structure of the meson vertices can be consistently taken into account which also defines the energy dependence of cross sections in the case of higher meson spins.

In Ref. [1] a reasonable description of the CLAS data on ρ^0 electroproduction has been obtained in the framework of a Regge model [15, 16] using the dominance of π , σ and f_2 trajectories. The tensor f_2 meson was implemented as an isoscalar meson with positive C -parity and $J = 1$ in accordance with the hypothesis that pomeron and f_2 trajectories are proportional. Also, an additional multiplier κ_{f_2} was introduced to rescale the contribution of the f_2 trajectory relative to the one of the pomeron. The

ρ^0 photoproduction [3]. As it turns out a significant enhancement of the f_2 trajectory contribution as compared to the pomeron trajectory ($\kappa_{f_2} = 9$) is required. The σ meson exchange has also been enhanced, because in [15] a large value for the $\rho\sigma\gamma$ coupling was used ($g_{\rho\sigma\gamma} \approx 1$, see details in [16]). Data on the $\rho \rightarrow \pi^0\pi^0\gamma$ decay width [20, 21] can be explained using a much smaller value for the $g_{\rho\sigma\gamma}$ coupling [20].

All this has been analyzed in Ref. [10] where the description of data on ρ photoproduction obtained earlier by [15] has been reconsidered. An alternative approach was proposed, where the amplitude of ρ^0 photoproduction was represented by the sum of the t -pole contributions from *physical* meson exchanges with coupling constants normalized to independent data (s - and u -pole contributions were taken into account as well). A good description of photoproduction data has been achieved in both approaches [15] and [10]. It seems that the σ and f_2 mesons showing up in the Regge model [15] are only *effective* degrees of freedom giving a useful parametrization of the total contribution by exchange of *physical* mesons listed in Table I.

In the present paper we also pursue an alternative description of the data on ρ^0 electroproduction similar to the approach of Ref. [10]. We start with phenomenological Lagrangians to calculate the cross sections σ_L and σ_T in the t -pole approximation for the set of mesons displayed in Table I (see also Fig.1). In our calculation we use the coupling constants and form factors supported by and deduced from data and which mostly coincide with those already used in Ref. [10] in the description of photoproduction data. The comparison of the theoretical results with latest data of the CLAS Collaboration [1] allows to determine the set of dominant meson exchanges corresponding to *physical* particles.

It will be found that in the description of the transverse cross section σ_T the pion contribution and the summed contribution of pseudovector mesons (f_1, f_1', a_1) and other pseudoscalars (η, η') in interference with the pion piece play the major role. In addition, the summed contribution of mesons with positive P -parity (f_0, f_2, a_0, a_2) is practically not visible in σ_T above such a background. In contrary, mesons with positive P -parity give a significant contribution to σ_L . However, if we use for all scalar f_0 mesons of Table I electromagnetic coupling constants $g_{\rho f_0\gamma}$ normalized to the known radiative decay widths of the σ and $f_0(980)$ mesons, the contribution of all f_0, a_0, f_2 and a_2 mesons will be not sufficient to explain the data on σ_L .

In the final part of the paper we discuss different scenarios for overcoming these difficulties. It is shown that the problem can be solved using the set of known scalar mesons (i.e. without inclusion of possible exotic states) if the set of heavy scalars ($f_0(1370)$, $f_0(1500)$ and $f_0(1710)$ or at least two states from this group) are considered as 3P_0 states in the $\bar{q}q$ spectrum. According to the quark model such states should have relatively large radiative

coupling constants $\rho f_0\gamma$ with $g_{\rho f_0\gamma} \gg g_{\rho\sigma\gamma}$ ($\bar{q}qg$ hybrid models with anomalous large widths [23] and models [24, 25] with large values for the $\rho\sigma\gamma$ or σNN coupling also do not contradict data, but one can proceed without these assumptions). Furthermore, in addition to the included σ meson exchange a non-correlated 2π exchange must also contribute to the cross section (recall that in Ref. [10] it was shown that this mechanism plays an appreciable role in the ρ^0 photoproduction at low energy).

We present our final results on the integrated $\sigma_{L/T}$ and differential $d\sigma_{L/T}/dt$ cross sections where the previously indicated corrections for the coupling constants $g_{\rho f_0\gamma}$ of two heavy mesons $f_0(1370)$ and $f_0(1500)$ are included. The results for $\sigma_{L/T}$ are compared to the latest data of the CLAS Collaboration [1, 2]. Theoretical curves are in agreement with data within experimental errors. The results for $d\sigma_{L/T}/dt$ appear to be in a good agreement with the new CLAS data [2] as illustrated for several experimental bins in the range of $1.9 < Q^2 < 2.2 \text{ GeV}^2/c^2$. A full analysis of all the experimental bins (more than 50 kinematical regions from $Q^2 = 1.6 \text{ GeV}^2/c^2$ and $x_B = 0.16$ to $Q^2 = 5.6 \text{ GeV}^2/c^2$ and $x_B = 0.7$) will be presented in a further paper in its own right.

II. FRAMEWORK

A. t -pole contributions due to exchange of mesons with positive C -parity

1. Scalar meson exchange ($S = f_0, a_0$)

We start with the effective Lagrangian

$$\mathcal{L}_{\rho S\gamma}(x) = \frac{e g_{\rho S\gamma}}{4M_\rho} S(x) F_{\mu\nu}(x) \rho^{\mu\nu}(x),$$

$$F_{\mu\nu} = \partial_\mu A_\nu - \partial_\nu A_\mu, \quad \rho_{\mu\nu} = \partial_\mu \rho_\nu - \partial_\nu \rho_\mu, \quad (1)$$

$$\mathcal{L}_{SNN}(x) = g_{SNN} S(x) \bar{N}(x) N(x) \quad (2)$$

which generates matrix elements due to the exchange of scalar mesons $S = f_0, a_0$. The respective invariant amplitude is

$$T_S(s, s', \lambda, \lambda_\rho) = e \frac{g_{\rho S\gamma}}{M_\rho} g_{SNN} \frac{g_{\mu\nu} k' \cdot q - k'_\nu q_\mu}{k^2 - M_{f_0}^2 + i0}$$

$$\times \epsilon_V^{(\lambda_\rho)\mu*}(k') \epsilon^{(\lambda)\nu}(q) \bar{u}(p', s') u(p, s), \quad (3)$$

where $\epsilon_V^{(\lambda)}(q)$ and $\epsilon_V^{(\lambda_\rho)}(k')$ are the polarization vectors of photon and ρ^0 meson, respectively. They satisfy completeness relations in the subspace orthogonal to the 4-momentum:

$$\sum_{\lambda=0,\pm 1} (-1)^\lambda \epsilon_\mu^{(\lambda)}(q) \epsilon_\nu^{(\lambda)*}(q) = g_{\mu\nu} - \frac{q_\mu q_\nu}{q^2},$$

$$\sum_{\lambda=0,\pm 1} \epsilon_\nu^{(\lambda_\rho)}(k') \epsilon_\mu^{(\lambda_\rho)*}(k') = - \left[g_{\mu\nu} - \frac{k'_\mu k'_\nu}{M^2} \right]. \quad (4)$$

Further, the invariant amplitude (3) is modified as usually by introducing vertex form factors

$$g_{\rho S\gamma} \rightarrow g_{\rho S\gamma} \mathcal{F}_{\rho S\gamma}(Q^2, t), \quad g_{SNN} \rightarrow g_{SNN} \mathcal{F}_{SNN}(t), \quad (5)$$

where

$$\mathcal{F}_{\rho S\gamma}(Q^2, t) \equiv \mathcal{F}_1(Q^2) \mathcal{F}_2(t), \quad \mathcal{F}_{SNN}(t) \equiv \mathcal{F}_3(t), \quad (6)$$

$t = k^2$ and $Q^2 = -q^2$. The substitution (5) is equivalent to a nonlocal form of the interaction vertices [26–28], i.e. to the following modification of the local Lagrangians (1) and (2):

$$\begin{aligned} \mathcal{L}_{\rho S\gamma}(x) &\rightarrow \mathcal{L}_{\rho S\gamma}^{NL}(x) = \frac{eg_{\rho S\gamma}}{4M_\rho} \int d^4y \int d^4z \Phi_1(z^2) \Phi_2(y^2) \\ &\quad \times S(x+y) F_{\mu\nu}(x+z) \rho^{\mu\nu}(x), \\ \mathcal{L}_{SNN}(x) &\rightarrow \mathcal{L}_{SNN}^{NL}(x) = g_{SNN} \int d^4y \Phi_3(y^2) \\ &\quad \times S(x+y) \bar{N}(x) N(x), \end{aligned} \quad (7)$$

where $\Phi_i(y^2)$ are relativistic invariant vertex functions. In momentum space $\mathcal{F}_i(k^2) = \int \Phi_i(y^2) e^{ik \cdot y} d^4y$ defines the corresponding vertex form factor.

The factors $g_{\rho f_0\gamma}$ and $\mathcal{F}_{\rho f_0\gamma}(Q^2, t)$ in the effective Lagrangian (1) should correspond to a specific physical process in the vertex. In particular, they should take into account the VMD transition $\gamma \rightarrow \rho^0$ with further diffractive scattering of the ρ^0 — in accordance with the diagram shown in Fig. 2a. An analogous process should contribute to the vertex $\rho\pi\gamma$ (see Fig. 2b) with the difference that here the spin $M1$ transition $\pi^0 \rightarrow \rho^0$ is understood. As a result the dependence of the form factors $\mathcal{F}_{\rho f_0\gamma}(Q^2, t)$ and $\mathcal{F}_{\rho\pi\gamma}(Q^2, t)$ on the virtuality Q^2 of the photon is described by the propagator of the vector meson $\frac{1}{Q^2 + M_\rho^2}$ in the first approximation. The dependence on t involves the specific scale Λ^{-1} corresponding to the size of the interaction volumes in the transitions $\rho^0 + f_0 \rightarrow \rho^0$ and $\omega + \pi \rightarrow \rho^0$ (see below).

The magnitudes of the $\rho S\gamma$ coupling constants can be estimated using the radiative decay width of the scalar meson f_0 with

$$\Gamma_{f_0 \rightarrow \gamma \rho} = \alpha \frac{g_{\rho f_0 \gamma}^2}{M_\rho^2} \left(\frac{M_{f_0}^2 - M_\rho^2}{2M_{f_0}} \right)^3, \quad (8)$$

while for the lightest scalar meson $f_0(600) \equiv \sigma$ the decay width for $\rho^0 \rightarrow \gamma + \sigma$

$$\Gamma_{\rho \rightarrow \gamma \sigma} = \frac{\alpha}{3} \frac{g_{\rho \sigma \gamma}^2}{M_\rho^2} \left(\frac{M_\rho^2 - M_\sigma^2}{2M_\rho} \right)^3 \quad (9)$$

is used. In Eqs. (8) and (9) we use coupling constants $g_{\rho f_0\gamma}$ fixed on the mass-shell ($Q^2 = 0, t = M_{f_0}^2$). Therefore, the form factor (5) for the $\rho f_0\gamma$ vertex must be normalized at $Q^2 = 0$ as

$$\mathcal{F}_{\rho f_0\gamma}(Q^2 = 0, t = M_{f_0}^2) = 1, \quad (10)$$

The σNN form factor is normalized according to

$$\mathcal{F}_{\sigma NN}(t = 0) = 1, \quad (11)$$

since the constant $g_{\sigma NN}$ is defined from NN scattering data at low energies in the limit $t \rightarrow 0$.

According to the data of the SND Collaboration [20] the width of ρ^0 decay into the channel with the lightest scalar meson σ is sufficiently large: $\Gamma_{\rho \rightarrow \gamma \sigma} \approx 2.83$ keV. Estimates of the decay width $\Gamma_{f_0 \rightarrow \gamma \rho}$ are also known for heavier scalar mesons, e.g. for $f_0(980)$ (~ 3.4 keV) obtained in the framework of the molecular $K\bar{K}$ model $f_0(980)$ [22, 29]. In both cases we obtain quite similar predictions for the coupling constants:

$$\begin{aligned} g_{\rho\sigma\gamma}/M_\rho &= 0.25/M_\rho = 0.32 \text{ GeV}^{-1}, \\ g_{\rho f_0\gamma}/M_\rho &\approx 0.21/M_\rho = 0.27 \text{ GeV}^{-1}. \end{aligned} \quad (12)$$

For the present purposes we use a unique value $g_{\rho\sigma\gamma} = 0.25$ for all scalar mesons in the calculation of the total exchange contribution involving $f_0(600)$, $f_0(980)$, $f_0(1370)$, $f_0(1500)$ and $f_0(1710)$.

Presently no data are available to constrain the $f_0 NN$ couplings except for the lightest scalar $\sigma = f_0(600)$. Here we take the value $g_{\sigma NN}^2/4\pi \simeq 4 \div 8$ commonly used in boson-exchange models of the NN interaction. As a rough estimate for of the contribution of the higher mass f_0 exchanges we use the common value $g_{f_0 NN} = g_{\sigma NN} = 10$. We note that σ_T is only weakly sensitive to even significant variation of the constants $g_{f_0 NN}$. Only σ_L allows to search for an averaged contribution of f_0 meson exchanges.

2. Pseudoscalar meson exchange ($S_5 = \pi^0, \eta, \eta'$)

The t -pole contribution due to pseudoscalar meson exchange is described as

$$\begin{aligned} T_{\pi^0}(s, s', \lambda, \lambda_\rho) &= -\frac{eg_{\rho\pi\gamma}}{2m_N M_\rho} \mathcal{F}_{\rho\pi\gamma}(Q^2, t) g_{\pi NN} \mathcal{F}_{\pi NN}(t) \\ &\quad \times \varepsilon^{\mu\nu\alpha\beta} \frac{\epsilon_\mu^{(\lambda)}(q) q_\nu \epsilon_{\nu\alpha}^{(\lambda_\rho)*}(k') k'_\beta}{M_\pi^2 - k^2 - i0} \bar{u}(p', s') \not{k} \gamma^5 u(p, s), \end{aligned} \quad (13)$$

where $g_{\rho\pi\gamma}$ and $g_{\pi NN}$ are the coupling constants related to the $\rho\pi\gamma$ and πNN vertices. The vertex $\rho\pi\gamma$ is generated by an effective Lagrangian with a minimal number of derivatives:

$$\mathcal{L}_{\rho\pi\gamma}(x) = \frac{eg_{\rho\pi\gamma}}{4M_\rho} \varepsilon^{\mu\nu\alpha\beta} F_{\mu\nu}(x) \vec{\rho}_{\alpha\beta}(x) \cdot \vec{\pi}(x). \quad (14)$$

For the πNN vertex we use a pseudovector coupling with $f_{\pi NN} = \frac{M_\pi}{2m_N} g_{\pi NN}$:

$$\mathcal{L}_{\pi NN}(x) = \frac{g_{\pi NN}}{2m_N} \bar{N}(x) \gamma^\mu \gamma^5 \vec{\pi} N(x) \cdot \partial_\mu \vec{\pi}(x). \quad (15)$$

The coupling constant $g_{\rho\pi\gamma}$ is deduced from the $\rho^0 \rightarrow \gamma + \pi^0$ decay width

$$\Gamma_{\rho \rightarrow \gamma \pi} = \frac{\alpha}{3} \frac{g_{\rho\pi\gamma}^2}{M_\rho^2} \left(\frac{M_\rho^2 - M_\pi^2}{2M_\rho} \right)^3. \quad (16)$$

With the experimental value of $\Gamma_{\rho \rightarrow \gamma \pi} = 93 \pm 19$ keV [21] we get

$$g_{\rho\pi\gamma}/M_\rho = 0.658/M_\rho = 0.848 \text{ GeV}^{-1}. \quad (17)$$

For the πNN coupling constant we use the standard value of $g_{\pi NN} = 13.4$.

For the η and η' mesons we have correspondingly:

$$\begin{aligned} g_{\rho\eta\gamma}/M_\rho &= 1.230/M_\rho = 1.585 \text{ GeV}^{-1}, \\ g_{\rho\eta'\gamma}/M_\rho &= 1.052/M_\rho = 1.356 \text{ GeV}^{-1}, \end{aligned} \quad (18)$$

using $\Gamma_{\rho \rightarrow \gamma \eta} = 45 \pm 3$ keV and $\Gamma_{\eta' \rightarrow \rho \gamma} = 60 \pm 6$ keV [21]. For the strong couplings $g_{\eta NN}$ and $g_{\eta' NN}$ the SU(3) relation is used

$$g_{\eta_8 NN} = \frac{3F - D}{\sqrt{3}(F + D)} g_{\pi NN} \quad (19)$$

for the mixing angle $\theta_P \approx -10^\circ$ [21] defining the state $\eta' = \eta_1 \cos \theta_P + \eta_8 \sin \theta_P$ (see e.g. Refs. [30, 31]). With $F/D = 0.575 \pm 0.016$ [32] we get

$$g_{\eta NN} = 4.38, \quad g_{\eta' NN} = 4.34, \quad (20)$$

where in addition we use the ratio $g_{\eta_1 NN} : g_{\eta_8 NN} = \sqrt{2} : 1$ which follows from a quark-model evaluation of the non-strange components in η_1 and η_8 .

3. Tensor meson exchange ($T = f_2, f_2', a_2$)

The Lagrangians for tensor meson interaction with nucleons and vector particles are constructed in the framework of tensor meson dominance (TMD) [9]. We follow Ref. [10] and only present necessary formulas for understanding the final results (see details in [10]).

The Lagrangian for a free tensor field $f_{\mu\nu}$ is described in the Fierz–Pauli framework and has a complicated form when external fields are included. However, the equations of motion are reduced to the usual Klein–Gordon equations for each independent component of the symmetric tensor field $f_{\alpha\beta} = f_{\beta\alpha}$:

$$(\partial_\mu^2 - M_T^2) f_{\alpha\beta} = 0 \quad (21)$$

with the additional constraints

$$\partial^\alpha f_{\alpha\beta} = 0, \quad g^{\alpha\beta} f_{\alpha\beta} = 0. \quad (22)$$

As result there are only 5 independent components of the

field has the form

$$G^{\alpha\beta; \alpha' \beta'}(k^2) = iP^{\alpha\beta; \alpha' \beta'}(k) \frac{1}{k^2 - M_T^2}, \quad (23)$$

$$P^{\alpha\beta; \alpha' \beta'}(k) = \frac{1}{2} \left(\bar{g}^{\alpha\alpha'} \bar{g}^{\beta\beta'} + \bar{g}^{\beta\alpha'} \bar{g}^{\alpha\beta'} \right) - \frac{1}{3} \bar{g}^{\alpha\beta} \bar{g}^{\alpha' \beta'},$$

$$\bar{g}^{\alpha\beta} = -g^{\alpha\beta} + \frac{k^\alpha k^\beta}{M_T^2}.$$

The electromagnetic vertex $\gamma^* + f_2 \rightarrow \rho^0$ depends on 4 Lorentz indices of the tensor and vector fields $f_{\alpha\beta}$, A_μ , ρ_ν and is described as a sum of two independent Lorentz-covariant terms with corresponding coupling constants $f_{\rho f_2 \gamma}$ and $g_{\rho f_2 \gamma}$ [9, 10]:

$$\begin{aligned} \Gamma^{\alpha\beta; \mu\nu}(k', q) &= \frac{e f_{\rho f_2 \gamma}}{M_{f_2}^2} \left[-g^{\mu\nu} q \cdot k' + k'^\nu q^\mu \right] \\ &\times (q + k')^\alpha (q + k')^\beta + e g_{\rho f_2 \gamma} \left[g^{\mu\nu} (q + k')^\alpha (q + k')^\beta \right. \\ &- g^{\mu\alpha} k'^\nu (q + k')^\beta - g^{\mu\beta} k'^\nu (q + k')^\alpha - g^{\nu\alpha} q^\mu (q + k')^\beta \\ &\left. - g^{\nu\beta} q^\mu (q + k')^\alpha + 2q \cdot k' (g^{\nu\alpha} g^{\mu\beta} + g^{\nu\beta} g^{\mu\alpha}) \right]. \end{aligned} \quad (24)$$

The strong coupling $f_2 NN$ also includes two independent Lorentz covariant terms:

$$\begin{aligned} \Gamma^{\alpha\beta}(p, p') &= \frac{G_{f_2 NN}}{m_N} [(p + p')^\alpha \gamma^\beta + (p + p')^\beta \gamma^\alpha] \\ &+ \frac{F_{f_2 NN}}{m_N^2} (p + p')^\alpha (p + p')^\beta. \end{aligned} \quad (25)$$

The magnitudes of the coupling constants $f_{\rho f_2 \gamma}$, $g_{\rho f_2 \gamma}$, $F_{f_2 NN}$ and $G_{f_2 NN}$ can be estimated in the framework of VMD and TMD models (see details in [9, 10]). In particular, the couplings are expressed in terms of two universal constants g_V and g_T :

$$\begin{aligned} e g_{\rho f_2 \gamma} &= e \frac{g_{f_2 V V}}{f_\rho M_{f_2}} = e \frac{g_T}{g_V M_{f_2}}, \quad G_{f_2 NN} = \frac{m_N}{2M_{f_2}} g_T, \\ f_{\rho f_2 \gamma} &= F_{f_2 NN} = 0, \end{aligned} \quad (26)$$

where $f_\rho = g_{\rho\pi\pi} = g_V$, $g_{f_2 V V} = g_{f_2 \pi\pi} = g_T$. The diagrams in Figs. 3 and 4 illustrate these conditions.

Tensor meson exchange contributions are described by the amplitude

$$\begin{aligned} T_{f_2}(s, s', \lambda, \lambda_\rho) &= \frac{2e g_{\rho f_2 \gamma} G_{f_2 NN}}{m_N (t - M_{f_2}^2)} \mathcal{F}_{\rho f_2 \gamma}(q^2, t) \mathcal{F}_{f_2 NN}(t) \\ &\times \bar{u}(p', s') \Gamma_{f_2} u(p, s), \end{aligned} \quad (27)$$

where

$$\begin{aligned} \Gamma_{f_2} &= (\epsilon_V^{(\lambda_\rho)})^* \epsilon^{(\lambda)} \left[((p+p')(q+k')) (\not{q} + \not{k}') \right. \\ &+ \frac{2m_N}{3} \left((q+k')^2 - \frac{1}{M_{f_2}^2} (k \cdot (q+k'))^2 \right) \\ &+ 2qk' \left[((p+p') \epsilon_V^{(\lambda_\rho)})^* \not{q}^{(\lambda)} + ((p+p') \epsilon^{(\lambda)}) \not{k}^{(\lambda_\rho)*} \right. \\ &\left. \left. + \frac{4m_N}{2} \left((\epsilon_V^{(\lambda_\rho)})^* \epsilon^{(\lambda)} - \frac{1}{M_{f_2}^2} (\epsilon_V^{(\lambda_\rho)})^* k \right) (\epsilon^{(\lambda)} k) \right) \right]. \end{aligned} \quad (28)$$

Here we introduced the vertex form factors $\mathcal{F}_{\rho f_2 \gamma}(q^2, t)$ and $\mathcal{F}_{f_2 NN}(t)$. These modify the constants $g_{\rho f_2 \gamma}$ and $G_{f_2 NN}$ in analogy with Eqs. (5)–(7) as:

$$\begin{aligned} g_{\rho f_2 \gamma} &\rightarrow g_{\rho f_2 \gamma} \mathcal{F}_{\rho f_2 \gamma}(Q^2, t), \\ G_{f_2 NN} &\rightarrow G_{f_2 NN} \mathcal{F}_{f_2 NN}(t). \end{aligned} \quad (29)$$

The values of these constants (see Fig. 4), $g_V = 5.33$ and $g_T = 5.76$, have been obtained using the decay data, $\Gamma_{\rho \rightarrow \pi\pi} = 150$ MeV and $\Gamma_{f_2 \rightarrow \pi\pi} = 156.5$ MeV [21], and the expressions:

$$\begin{aligned} \Gamma_{\rho^0 \rightarrow \pi\pi} &= \frac{g_V^2}{4\pi} \frac{M_\rho}{12} \left(1 - \frac{4M_\pi^2}{M_\rho^2}\right)^{3/2}, \\ \Gamma_{f_2 \rightarrow \pi\pi} &= \frac{g_T^2}{4\pi} \frac{M_f}{20} \left(1 - \frac{4M_\pi^2}{M_f^2}\right)^{5/2}. \end{aligned} \quad (30)$$

Here we suppose ideal mixing between $f_2(1270)$ and $f_2'(1525)$. This means that the coupling of $f_2'(1525)$ to the $\pi\pi$ channel is suppressed by the Okubo, Zweig and Iizuka rule as observed in experiment [21]. Therefore, in the first approximation one can neglect the contribution of $f_2'(1525)$ in the electroproduction of ρ^0 .

4. Axial-vector meson exchange ($V_5 = f_1, f_1', a_1$)

Considering the $J^{PC} = 1^{++}$ particle V_5 as a quark-antiquark 3P_1 bound state one can write the coupling $1^{++} \rightarrow \gamma^*(q)V(k')$ in a form analogous to the ${}^3P_1 \rightarrow \gamma^*\gamma^*$ coupling calculated in the quark model (see, e.g. [33]):

$$\begin{aligned} \mathcal{M}(1^{++} \rightarrow \gamma^*V) &= \epsilon_{\nu\nu}^{(\lambda\rho)*} \Gamma_{V_5}^{\alpha,\mu\nu} \epsilon_\mu^{(\lambda)} \epsilon_{V_5\alpha}, \\ \Gamma_{V_5}^{\alpha,\mu\nu} &= e g_{\rho V_5 \gamma} \varepsilon^{\mu\nu\alpha\beta} \frac{k'^2 q_\beta - q^2 k'_\beta}{M^2}, \quad q^\mu \epsilon_\mu^{(\lambda)}(q) = 0 \end{aligned} \quad (31)$$

($V = \rho^0$ and $\epsilon_{V_5\alpha}$ is the polarization vector of V_5). Here it is implied that the radial derivative $R'_{q\bar{q}}(0)$ of the $q\bar{q}$ wave function is included to the constant $g_{\rho V_5 \gamma}$ and the coupling can be further modified by a form factor.

Starting with this analogy we introduce the interaction Lagrangian

$$\begin{aligned} \mathcal{L}_{\rho V_5 \gamma}(x) &= e \frac{g_{\rho V_5 \gamma}}{M_\rho^2} \varepsilon^{\mu\nu\alpha\beta} V_{5\alpha} (\partial_\beta A_\mu \square \rho_\nu \\ &\quad - \partial_\beta \rho_\nu (g_{\mu\mu'} \square - \partial_\mu \partial_{\mu'}) A^{\mu'}) \end{aligned} \quad (32)$$

$$\mathcal{L}_{V_5 NN}(x) = g_{V_5 NN} \bar{N}(x) \gamma^\alpha \gamma^5 N(x) V_{5\alpha}(x), \quad (33)$$

and write down the t -pole axial-vector meson contribu-

factors:

$$\begin{aligned} T_{V_5}(s, s', \lambda, \lambda_\rho) &= -e g_{\rho V_5 \gamma} g_{V_5 NN} \mathcal{F}_{\rho V_5 \gamma}(q^2, t) \mathcal{F}_{V_5 NN}(t) \\ &\times \varepsilon^{\mu\nu\alpha\beta} \left(q_\nu - \frac{q^2}{M_\rho^2} k'_\nu \right) \epsilon_\mu^{(\lambda)}(q) \epsilon_{V_5\alpha}^{(\lambda_\rho)*}(k') \\ &\times \frac{g_{\beta\beta'} - k_\beta k_{\beta'}/M_f^2}{k^2 - M_f^2} \bar{u}(p', s') \gamma^{\beta'} \gamma^5 u(p, s). \end{aligned} \quad (34)$$

On this basis the radiative decay $f_1 \rightarrow \gamma\rho$ width is calculated as:

$$\Gamma_{f_1 \rightarrow \gamma\rho} = \frac{\alpha}{3} \frac{g_{\rho f_1 \gamma}^2}{M_\rho^2} \left(1 + \frac{M_\rho^2}{M_{f_1}^2}\right) \left(\frac{M_{f_1}^2 - M_\rho^2}{2M_{f_1}}\right)^3. \quad (35)$$

Using the experimental value $\Gamma_{f_1 \rightarrow \gamma\rho} = 1.34 \pm 0.32$ MeV [21] we get:

$$\begin{aligned} g_{\rho f_1 \gamma}/M_\rho &= 1.901/M_\rho = 2.45 \text{ GeV}^{-1}, \\ g_{\rho f_1' \gamma}/M_\rho &= 0.582/M_\rho = 0.748 \text{ GeV}^{-1}. \end{aligned} \quad (36)$$

To get $g_{\rho f_1' \gamma}$ we have used quark counting [34] for the matrix element of the charge operator

$$e_q = \sum_i \left(\frac{1}{2} \lambda_3^{(i)} + \frac{1}{2\sqrt{3}} \lambda_8^{(i)} \right) \quad (37)$$

in neutral meson–meson transitions of opposite C -parity (in our case we deal with the transitions $f_1 \rightarrow \rho^0$, $f_1' \rightarrow \rho^0$ and $a_1 \rightarrow \rho^0$). The dependence of the matrix element on the isospin part of the meson (f_n or a_n) wave function is described by the simple relations [34]:

$$\begin{aligned} \langle f_n(I=0) | e_q | a_n(I=1) \rangle &= 1, \\ \langle f_n(I=1) | e_q | f_n(I=1) \rangle &= \frac{1}{3}, \\ \langle a_n(I=0) | e_q | a_n(I=0) \rangle &= \frac{1}{3}. \end{aligned} \quad (38)$$

The final results for the $f_1(1285)$ and $f_1'(1410)$ mesons

$$\begin{aligned} \langle \rho^0 | e_q | f_1' \rangle / \langle \rho^0 | e_q | f_1 \rangle &= \sin \epsilon / \cos \epsilon, \\ g_{\rho f_1' \gamma} &= g_{\rho f_1 \gamma} \tan \epsilon \end{aligned} \quad (39)$$

only depend on the mixing angle $\epsilon \approx 17^\circ$ [35] relating nonstrange and strange components in the initial meson (the final meson is the isovector $\rho^0 = (\bar{u}u - \bar{d}d)/\sqrt{2}$) with

$$\begin{aligned} f_1(1285) &= \cos \epsilon \frac{\bar{u}u + \bar{d}d}{\sqrt{2}} - \sin \epsilon \bar{s}s, \\ f_1(1410) &= \sin \epsilon \frac{\bar{u}u + \bar{d}d}{\sqrt{2}} + \cos \epsilon \bar{s}s. \end{aligned} \quad (40)$$

For the axial-vector isovector meson $a_1(1260)$ the corresponding coupling in the electromagnetic transition $a_1 + \gamma \rightarrow \rho^0$ can be expressed through the constant $g_{\rho f_1 \gamma}$ also using relations (38): $g_{\rho a_1 \gamma} = \frac{1}{3} g_{\rho f_1 \gamma}$. This is also fulfilled for any type of $f_n(a_n)$ meson considered here and we accept

$$g_{\rho f_n \gamma} = \frac{1}{3} g_{\rho f_1 \gamma}, \quad n = I = 0, 1, 2 \quad (41)$$

In Ref. [36] an estimate for the couplings of the $f_1(1285)$ and $f_1'(1410)$ mesons to nucleons was obtained using the hypothesis of partial conservation of the axial-vector current, i.e. in analogy to the VMD model, which in this case is extended to neutral axial-vector mesons. According to Ref. [36] $|g_{f_1 NN}| = 1.46$ and $|g_{f_1' NN}| = 10.5$. If the neutral axial-vector current is only connected to the strange component in the nucleon [36, 37] then, following (40), it follows that these couplings have different signs and we use the values

$$g_{f_1 NN} = -1.46, \quad g_{f_1' NN} = 10.5. \quad (42)$$

B. Form factors

Finally in this section we make a few comments concerning the vertex form factors $\mathcal{F}_{\rho M \gamma}$ and $\mathcal{F}_{M NN}$ showing up in expression for \mathcal{N}_M (see Table III). In the calculations we use a common monopole form factor describing the dependence on the virtuality of the (absorbed) particle in the case that the other two are on the mass shell:

$$\begin{aligned} \mathcal{F}_{\gamma M \rho^0}(Q^2, t = M_M^2) &= \frac{\Lambda_q^2}{\Lambda_q^2 + Q^2}, \\ \mathcal{F}_{M NN}(t) &= \frac{\Lambda_t^2}{\Lambda_t^2 - t}, \quad \Lambda_t = \Lambda_q = M_\rho. \end{aligned} \quad (43)$$

For the upper vertex in the diagrams of Fig.2 this form factor is the propagator of the virtual vector meson in the VMD. The same is also true for the form factors in the upper vertex of the analogous diagram of Fig.1. In the interpretation of the form factor as the Fourier transform of the function $\Phi(y^2)$ (describing a nonlocal interaction in (7)) the expression of Eq. (43) takes only into account the characteristic scale $\sim \frac{1}{\Lambda} \approx \frac{1}{M_\rho}$ of the charge distribution of (any sort) in the hadron (but this is quite sufficient for our purposes). This procedure is also based on a similar description for quasi-elastic knockout of pions on the nucleon [7, 19] with similar kinematics. The corresponding magnitude of Λ_t is correlated with data on π^+ electroproduction [4–6].

If a vertex in the diagram contains two off-shell particles (as is the case for the upper vertex in the diagrams of Figs. 1 and 2), then a form factor should depend on both virtualities: $t - M_M^2$ and Q^2 . In the case of pion exchange in the quasi-elastic knockout ($t \approx 0$) the virtuality on t is negligible $M_\pi^2 - t \approx 0$ and the t -dependence in the $\gamma \pi \rho$ vertex can be neglected. However, in case of heavy meson exchange $M = f_0(a_0), f_1(a_1), f_2(a_2)$ we cannot neglect the dependence on the virtuality $t - M_M^2$ for typical values of the momentum transfer squared $t \approx t_{min}$ in quasi-elastic knockout. Therefore we use for the $\gamma M \rho$ form factor a more complicated parametrization:

$$\mathcal{F}_{\gamma M \rho^0}(Q^2, t) = \frac{\Lambda_q^2}{\Lambda_q^2 + Q^2} \frac{\Lambda_0^2}{\Lambda_0^2 + M_M^2 - t}, \quad (44)$$

Here the second factor is normalized to 1 for $t = M_M^2$ — in correspondence with the normalization of the coupling $\gamma M \rho^0$ for the observable decay widths chosen in Eqs. (8) - (12), (30) and (35) - (36). We use in the form factor (44) the same value for the cutoff $\Lambda_0^2 = 1.2 \text{ GeV}^2/c^2$ as in Ref. [7]. There we showed that such a parametrization is successful to describe data on the electroproduction of pions [4–6] in the framework of an analogous t -pole mechanism with the off-shell $\gamma \rho \pi$ coupling.

In the literature the t -dependence of the form factor (44) is usually represented in the form $\frac{\tilde{\Lambda}_0^2 - M_M^2}{\tilde{\Lambda}_0^2 - t}$ with approximately the same value for $\tilde{\Lambda}_0 \approx 1.2\text{--}1.5 \text{ GeV}/c$. For a relatively small value of the meson mass $M_M \lesssim 1 \text{ GeV}$ in expression (44) both parametrizations lead to approximately the same results in the considered region $t \sim 0$. For more massive mesons $M_M \gtrsim 1.3\text{--}1.5 \text{ GeV}$ the value of $\tilde{\Lambda}_0$ will depend on the meson mass. To avoid the introduction of new free parameters we use the parametrization (44) for all the $f_0(a_0)$ and $f_1(a_1)$ mesons. Only in the case of the f_2 meson we keep the standard parametrization (for the value of $\Lambda_{f_2} = 1.4 \text{ GeV}/c$),

$$\begin{aligned} \mathcal{F}_{\gamma f_2 \rho^0}(Q^2, t) &= \frac{\Lambda_q^2}{\Lambda_q^2 + Q^2} \frac{\Lambda_{f_2}^2 - M_{f_2}^2}{\Lambda_{f_2}^2 - t}, \\ \mathcal{F}_{f_2 NN}(t) &= \frac{\Lambda_{f_2}^2 - M_{f_2}^2}{\Lambda_{f_2}^2 - t}, \end{aligned} \quad (45)$$

which was already used by other authors (see e.g. Ref. [10] and references therein).

III. ELECTROPRODUCTION CROSS SECTION: TRANSVERSE AND LONGITUDINAL PARTS

Recent experiments of the CLAS [1, 2, 38] and F_π [4–6] Collaborations at JLAB on meson electroproduction in the quasi-elastic region allow in principle to separate individual meson exchange contributions. Therefore the corresponding electromagnetic and strong vertex form factors can be measured directly. In particular, in the CLAS experiments [1, 2, 4–6] the differential cross section of meson electroproduction is separated in longitudinal (L), transverse (T) and mixed (TT , LT) parts as

$$\begin{aligned} \frac{d^4 \sigma}{dW^2 dQ^2 dt d\varphi_{M'}} &= \Gamma \left\{ \varepsilon \frac{d\sigma_L}{dt} + \frac{d\sigma_T}{dt} + \varepsilon \frac{d\sigma_{TT}}{dt} \cos 2\varphi_{M'} \right. \\ &\quad \left. + \sqrt{2\varepsilon(1+\varepsilon)} \frac{d\sigma_{LT}}{dt} \cos \varphi_{M'} \right\} \end{aligned} \quad (46)$$

by varying ε and $\varphi_{M'}$ (via the Rosenbluth separation).

In Eq. (46) W^2 is the square of the invariant mass with $W^2 = s = (q + p)^2 = (k' + p')^2$; p and p' are the 4-momenta of the target and recoil nucleon respectively, k' is the 4-momentum of the produced meson M' and q is the 4-momentum of the virtual photon $q = (q_0, \mathbf{q})$ (see Fig. 1) with $Q^2 = -q^2$; $t = (p' - p)^2 = (k' - q)^2 = k^2$

is the angle between the electron scattering plane and the plane spanned by the $(\mathbf{k}', \mathbf{p}')$ momenta; the value of $\Gamma = \frac{1}{(4\pi)^2} \frac{W^2 - m_N^2}{Q^2 E_e^2 m_N^2} \frac{1}{1 - \varepsilon}$ is the virtual photon flux. Here E_e is the initial electron energy and $\varepsilon = \left[1 + \frac{2q^2 \tan^2 \frac{\theta_e}{2}}{Q^2}\right]^{-1}$ characterizes the degree of longitudinal polarization of the virtual photon (θ_e is the angle between the momenta of the incident and scattered electrons).

This separation permits to determine the contributions of π and ρ meson poles in the cross section of pion electroproduction ($M' = \pi^+$) [7]. In the reaction $p(e, e'\rho^0)p$ the Rosenbluth separation (46) ($M' = \rho^0$) also increases the chances (in comparison to older less precise data [8]) to determine the contribution e.g. of the pion pole (see below).

In this section we derive and present the formula for the individual contribution of each meson exchange considered to the longitudinal and transverse part of the cross section (also including the interference terms) using the previously shown amplitudes with a fixed photon polarization $\lambda = 0, \pm 1$.

We start from the full amplitude as a sum of t -pole contributions of isoscalar (f_n) and isovector (a_n) mesons

$$T(s, s', \lambda, \lambda_\rho) = \sum_{f_n, a_n} (T_S + T_{S_5} + T_{V_5} + T_T), \quad (47)$$

containing the expressions (3), (13), (27) and (34) obtained in the previous section. The original expression for the t -pole amplitude T_M corresponding to the exchange of meson $M = S, S_5, V_5, T$ is written in general form as

$$T_M(s, s', \lambda, \lambda_\rho) = \epsilon_\nu^{(\lambda\rho)}(k')^* \Gamma_M^{\varkappa, \mu\nu} \epsilon_\mu^{(\lambda)}(q) G_M^{\varkappa, \varkappa'}(k) \times \bar{u}(p', s') \Gamma_M^{\varkappa'} u(p, s), \quad (48)$$

where $\Gamma_M^{\varkappa, \mu\nu}$ and $\Gamma_M^{\varkappa'}$ are expressions for the $\rho M \gamma$ and $M N N$ vertices respectively (see Table II) and $G_M^{\varkappa, \varkappa'}(k)$ is the meson propagator. Here it is understood that the index \varkappa encodes the Lorentz indices of the exchanged meson M , i.e. $\varkappa = \alpha$ for $M = V_5$ (see Eq. (31)), $\varkappa = \alpha\beta$ for $M = T$, while the \varkappa is omitted in the case of $M = S, S_5$.

After averaging and summing the probability $|T|^2$ over all polarizations (excluding the polarization λ of the initial photon) with

$$\overline{|T^{(\lambda)}|^2} = \frac{1}{2} \sum_{s, s', \lambda_\rho} T(s, s', \lambda, \lambda_\rho) T^*(s, s', \lambda, \lambda_\rho) \quad (49)$$

in the Rosenbluth formula are reduced to the form:

$$\begin{aligned} \frac{d\sigma_L}{dt} &= \mathcal{N} \frac{1}{4\pi} \overline{|T^{(\lambda=0)}|^2}, \\ \frac{d\sigma_T}{dt} &= \mathcal{N} \frac{1}{2} \sum_{\lambda=\pm 1} \frac{1}{4\pi} \overline{|T^{(\lambda)}|^2}, \\ \frac{d\sigma_{TT}}{dt} &= \mathcal{N} \left\{ -\frac{1}{2} \sum_{\lambda=\pm 1} \frac{1}{4\pi} \overline{T^{(\lambda)} T^{(-\lambda)*} } \right\}, \\ \frac{d\sigma_{LT}}{dt} &= \mathcal{N} \left\{ -\frac{1}{2} \sum_{\lambda=\pm 1} \lambda \left(\frac{\overline{T^{(0)} T^{(\lambda)*} + \overline{T^{(\lambda)} T^{(0)*}}}{4\pi\sqrt{2}} \right) \right\}. \end{aligned} \quad (50)$$

Here we introduce the standard constant

$$\mathcal{N} = \left[2m_N Q \sqrt{1 + \left(\frac{W^2 - m_N^2 + Q^2}{2m_N Q} \right)^2} (W^2 - m_N^2) \right]^{-1}$$

corresponding to the normalization of the cross section to unit flow of virtual photons.

The individual meson $M = f_n, a_n$ contributions to the cross section (50) can be presented in a general form — in the form of products of the polarization vectors $\epsilon_\mu^{(\lambda)} \epsilon_{\mu'}^{(\lambda)*}$, with five independent tensors: $k^\mu k^{\mu'}$, $p^\mu p^{\mu'}$, $p^\mu k^{\mu'} + k^\mu p^{\mu'}$, $g^{\mu\mu'}$ and $\varepsilon^{\mu\nu\alpha\beta} \varepsilon_{\mu'\nu'\alpha'\beta'} q_\nu q_{\nu'} k_\alpha k_{\alpha'} p_\beta p_{\beta'}$ (tensors of the form $q^\mu k^{\mu'}$, $q^\mu p^{\mu'}$, etc. can be omitted because of the condition $q^\mu \epsilon_\mu^{(\lambda)} = 0$). In the lab frame with $p^\mu = \{m_N, 0, 0, 0\}$ the latter tensor, after contraction with $\epsilon_\mu^{(\lambda)} \epsilon_{\mu'}^{(\lambda)*}$, is transformed into the mixed product of 3-vectors:

$$\begin{aligned} &\left\{ \varepsilon^{\mu\nu\alpha\beta} \varepsilon_{\mu'\nu'\alpha'\beta'} \epsilon_\mu^{(\lambda)} \epsilon_{\mu'}^{(\lambda)*} q_\nu q_{\nu'} k_\alpha k_{\alpha'} p_\beta p_{\beta'} \right\}_{\text{lab}} \\ &= \lambda^2 m_N^2 ([\mathbf{q} \times \mathbf{k}] \cdot \boldsymbol{\epsilon}^{(\lambda)}) ([\mathbf{q} \times \mathbf{k}] \cdot \boldsymbol{\epsilon}^{(\lambda)*}). \end{aligned} \quad (51)$$

Using the tensor decomposition we obtain the following expression for the individual contribution of meson M :

$$\begin{aligned} \overline{|T_M^{(\lambda)}|^2} &\equiv \frac{1}{2} \sum_{s, s'} \sum_{\lambda_\rho} |T_M(s, s', \lambda, \lambda_\rho)|^2 \\ &= \mathcal{N}_M^2 \left\{ A_M (\epsilon^{(\lambda)} \epsilon^{(\lambda)*}) + B_M \frac{1}{m_N^2} (k\epsilon^{(\lambda)}) (k\epsilon^{(\lambda)*}) \right. \\ &+ C_M \frac{1}{m_N^2} (p\epsilon^{(\lambda)}) (p\epsilon^{(\lambda)*}) \\ &+ D_M \frac{1}{m_N^2} [(p\epsilon^{(\lambda)}) (k\epsilon^{(\lambda)*}) + (k\epsilon^{(\lambda)}) (p\epsilon^{(\lambda)*})] \\ &\left. + E_M \frac{1}{m_N^4} [\mathbf{k} \times \mathbf{q}] \cdot \boldsymbol{\epsilon}^{(\lambda)} [\mathbf{k} \times \mathbf{q}] \cdot \boldsymbol{\epsilon}^{(\lambda)*} \right\}, \end{aligned} \quad (52)$$

where the coefficients A_M, B_M, C_M, D_M and E_M are functions of three independent invariants $t = k^2, Q^2 = -q_\mu^2$ and $s = (p + q)^2 = W^2$. The full expressions are given in Table III and in the Appendix.

We use dimensionless invariant variables

$$\begin{aligned} \xi_s &\equiv \frac{pq}{m_N Q} = \frac{W^2 - m_N^2 + Q^2}{2m_N Q}, \\ \xi_t &\equiv \frac{kq}{m_N Q} = \frac{-t + M_\rho^2 + Q^2}{2m_N Q}, \quad \eta = \frac{-t}{m_N Q}, \end{aligned} \quad (53)$$

in terms of which the coefficients A_M , B_M , C_M and D_M can be expressed in the simplest form. Parameter ξ_s has a simple physical meaning because it is proportional to the inverse of the Bjorken variable $x_B = \frac{Q^2}{2pq} = \frac{Q}{2m_N \xi_s}$ (here the parameter ξ_t has an analogous meaning in the t channel for the virtual meson M). The factor \mathcal{N}_M , given in the last line of Table III, depends on the coupling constants, form factors and the meson propagator.

The interference terms have the same parametrization as the diagonal terms:

$$\begin{aligned}
& \overline{T_M^{(\lambda)} T_{M'}^{(\lambda)*} + T_{M'}^{(\lambda)} T_M^{(\lambda)*}} \\
& \equiv \frac{1}{2} \sum_{ss'} \sum_{\lambda\rho} \left[T_M(s, s', \lambda, \lambda_\rho) T_{M'}^*(s, s', \lambda, \lambda_\rho) \right. \\
& + \left. T_{M'}(s, s', \lambda, \lambda_\rho) T_M^*(s, s', \lambda, \lambda_\rho) \right] = \mathcal{N}_M \mathcal{N}_{M'} \\
& \times \left\{ A_{MM'} (\epsilon^{(\lambda)} \epsilon^{(\lambda)*}) + B_{MM'} \frac{1}{m_N^2} (k\epsilon^{(\lambda)})(k\epsilon^{(\lambda)*}) \right. \\
& + C_{MM'} \frac{1}{m_N^2} (p\epsilon^{(\lambda)})(p\epsilon^{(\lambda)*}) \\
& + D_{MM'} \frac{1}{m_N^2} [(p\epsilon^{(\lambda)})(k\epsilon^{(\lambda)*}) + (k\epsilon^{(\lambda)})(p\epsilon^{(\lambda)*})] \\
& \left. + E_{MM'} \frac{1}{m_N^4} [\mathbf{k} \times \mathbf{q}] \cdot \epsilon^{(\lambda)} [\mathbf{k} \times \mathbf{q}] \cdot \epsilon^{(\lambda)*} \right\} \quad (54)
\end{aligned}$$

and vanish for mesons of opposite parity after averaging over the polarizations λ_ρ, s, s' . We therefore consider only the two nontrivial contributions for $MM' = ST$ and $MM' = S_5V_5$. The corresponding coefficients A, B, C, D and E are given in Table IV.

Such a form of the final results has to simplify the calculation of $\sigma_{L(T)}$ — one only substitutes the following expressions into the r.h.s. of Eqs. (52) and (54):

1) For σ_L ($\lambda = 0$)

$$\begin{aligned}
& (\epsilon^{(\lambda=0)} \epsilon^{(\lambda=0)}) = 1, \\
& \frac{1}{m_N^2} (k\epsilon^{(\lambda=0)})(k\epsilon^{(\lambda=0)*}) = \frac{(-2\eta + \xi_s \xi_t)^2}{1 + \xi_s^2} \\
& = (\xi_t^2 - 4\eta) + \frac{\mathbf{k}_{\text{lab}}^2}{m_N^2} \sin^2 \theta_k^{\text{lab}}, \\
& \frac{1}{m_N^2} (p\epsilon^{(\lambda=0)})(p\epsilon^{(\lambda=0)*}) = (1 + \xi_s^2), \\
& \frac{1}{m_N^2} \left[(p\epsilon^{(\lambda=0)})(k\epsilon^{(\lambda=0)*}) + (p\epsilon^{(\lambda=0)*})(k\epsilon^{(\lambda=0)}) \right] \\
& = 2(-2\eta + \xi_s \xi_t), \\
& \frac{1}{m_N^4} ([\mathbf{q} \times \mathbf{k}] \cdot \epsilon^{(\lambda=0)}) ([\mathbf{q} \times \mathbf{k}] \cdot \epsilon^{(\lambda=0)*}) = 0. \quad (55)
\end{aligned}$$

2) For σ_T ($\lambda = \pm 1$)

$$\begin{aligned}
& \frac{1}{2} \sum_{\lambda=\pm 1} (\epsilon^{(\lambda)} \epsilon^{(\lambda)*}) = -1, \\
& \frac{1}{2} \sum_{\lambda=\pm 1} \frac{1}{m_N^2} (k\epsilon^{(\lambda)})(k\epsilon^{(\lambda)*}) = \frac{\mathbf{k}_{\text{lab}}^2}{2m_N^2} \sin^2 \theta_k^{\text{lab}}, \\
& \frac{1}{2} \sum_{\lambda=\pm 1} \frac{1}{m_N^2} (p\epsilon^{(\lambda)})(p\epsilon^{(\lambda)*}) = 0, \\
& \frac{1}{2} \sum_{\lambda=\pm 1} \frac{1}{m_N^2} \left[(p\epsilon^{(\lambda)})(k\epsilon^{(\lambda)*}) + (p\epsilon^{(\lambda)*})(k\epsilon^{(\lambda)}) \right] = 0, \\
& \frac{1}{2} \sum_{\lambda=\pm 1} \frac{1}{m_N^4} ([\mathbf{q} \times \mathbf{k}] \cdot \epsilon^{(\lambda)}) ([\mathbf{q} \times \mathbf{k}] \cdot \epsilon^{(\lambda)*}) \\
& = (1 + \xi_s^2) \frac{Q^2}{m_N^2} \frac{\mathbf{k}_{\text{lab}}^2}{2m_N^2} \sin^2 \theta_k^{\text{lab}}. \quad (56)
\end{aligned}$$

Here we use the lab frame ($\mathbf{p} = 0$) with the z axis parallel to the photon momentum \mathbf{q} . Then the square of the 3-momentum \mathbf{k} and the energy k_0 of the virtual meson M have the forms: $\mathbf{k}^2 = 4m_N^2 \eta(1 + \eta)$ and $k_0 = \frac{t}{2m_N} = -2m_N \eta$. The polar angle $\theta_M = \theta_k^{\text{lab}}$ of the virtual meson 3-momentum is only used as a variable in Eqs. (55) - (56). It is expressed by values of the dimensionless parameters ξ_s, ξ_t and η as

$$\begin{aligned}
\frac{\mathbf{k}^2}{m_N^2} \sin^2 \theta_k^{\text{lab}} &= \frac{4\eta(1 + \eta + \xi_s^2 - \xi_s \xi_t) - \xi_t^2}{1 + \xi_s^2}, \\
\frac{|\mathbf{k}|}{m_N} \cos \theta_k^{\text{lab}} &= -\frac{(\xi_t + 2\eta \xi_s)}{\sqrt{1 + \xi_s^2}}. \quad (57)
\end{aligned}$$

The momentum \mathbf{k}' and the polar angle θ'_ρ of the emitted ρ^0 meson can be related to the variables \mathbf{k} and θ_k^{lab} using the following relations:

$$\begin{aligned}
\mathbf{k}'^2 \sin^2 \theta'_\rho &= \mathbf{k}^2 \sin^2 \theta_k^{\text{lab}}, \\
|\mathbf{k}'| \cos \theta'_\rho &= |\mathbf{q}| + |\mathbf{k}| \cos \theta_k^{\text{lab}}, \quad (58)
\end{aligned}$$

where it is understood that in the lab frame $|\mathbf{q}| = Q\sqrt{1 + \xi_s^2}$, $q_0 = Q\xi_s$, $k'_0 = Q\xi_s - 2m_N \eta$ and $\mathbf{k}'^2 = k'_0{}^2 - M_\rho^2$.

IV. RESULTS AND DISCUSSION

Results for the cross sections $\sigma_{L(T)}$ of ρ^0 electroproduction in comparison with the data of the CLAS Collaboration [1] are presented in Fig. 5 — separately for transverse (right side) σ_T and for longitudinal (left side) σ_L parts. For $W \gtrsim 2$ GeV (i.e. at $x_B = 0.31$ and 0.38 in the CLAS kinematics) the underlying mechanism of quasi-elastic meson knockout (quark spin-flip in the $M1$ transitions $\gamma_T^* + \pi^0(\eta, \eta') \rightarrow \rho^0$ and change of internal orbital momentum in the $E1$ transitions $\gamma_T^* + f_n(a_n) \rightarrow \rho^0$, $n = 0.1, 2$) summed over all meson exchange contributions [see Table I, including the ρ exchange contribution in the t channel]

the data on $\sigma_T(Q^2, W)$. However, there is no such agreement for σ_L . As seen from Fig. 5 for σ_T the pion exchange contribution is enhanced due to the interference with the exchanged contributions of other pseudoscalar ($S_5 = \eta, \eta'$) and axial-vector ($V_5 = f_1, f_1', a_1$) mesons (curves with short-dashed lines in Figs. 5, 6 and 8) while it is suppressed in σ_L . It seems that a full explanation of the large value of σ_L is based on another reaction mechanism.

We therefore conclude that the mechanism of quasi-elastic meson knockout from the nucleon cloud (with the conversion $M_5 \rightarrow \rho^0$) is only weakly realized in the longitudinal cross section. At the same time, electroproduction through scalar f_0 meson exchange could be connected to another – diffractive – mechanism (see Fig. 2a). It seems that in this case the couplings $\rho f_0 \gamma$ for different f_0 mesons must be such that their total contribution to the longitudinal part σ_L is equivalent to the contribution of the diffractive mechanism. However, as seen from the results displayed in Fig. 5 the total contribution of five f_0 mesons, further enhanced because of interference with the other mesons f_2, a_0, a_2 of positive parity (curves with long-dashed lines in Fig. 5), is not enough to reproduce the data on σ_L .

The mismatch of theory with data on σ_L is perhaps connected with the fact that for all five f_0 mesons we use a universal $\rho f_0 \gamma$ constant $g_{\rho f_0 \gamma}$ justified only for the radiative decay widths of the lightest scalars: $f_0(980) \rightarrow \rho^0 + \gamma$ and $\rho^0 \rightarrow \sigma + \gamma$. The value used here $g_{\rho f_0 \gamma} = 0.25$ corresponds to a typical scale of electromagnetic interactions of the f_0 meson interpreted as a weakly bound molecular $K\bar{K}$ state (in case of $f_0(980)$) [22, 29] or as coupled channel state $\pi\bar{\pi} + q\bar{q}$ with a dominant $\pi\bar{\pi}$ component (in case of the $\sigma = f_0(600)$) [39]. Then there must be further scalar states with the $q\bar{q}$ component as the dominant one. In many studies (see, e.g. [23, 29, 34, 40, 41]) the heavy scalar mesons $f_0(1370)$, $f_0(1500)$ and $f_0(1710)$ are interpreted as either $q\bar{q}$ 3P_0 states or as a mixed state including an additional glueball G_J , $J = 0$ with mass ~ 1.7 GeV according to lattice calculations [42].

In the classification of the scalar mesons we follow the $SU(3)_F \times O(3)$ scheme of Table I. We adopt the view that the lowest scalar nonet [$\sigma(600)$, $f_0(980)$, $a_0(980)$, $\kappa(800)$] is described by four-quark(antiquark) S -wave configurations $q^2\bar{q}^2$ which are strongly coupled to the open 2π , $2K$ and πK channels. For the lowest-lying 3P_0 nonet of the $q\bar{q}$ system we use the scalar states with their masses close to the averaged mass of the other $^3P_{J=1,2}$ nonets [i.e. to the masses of $f_1(1285)$, $f_1'(1420)$, $f_2(1270)$, $f_2'(1525)$, ..., etc.]. Since the 3P_0 nonet can accommodate only two isoscalar-scalar f_0 configurations only two of the three observed resonances, $f_0(1370)$, $f_0(1500)$ and $f_0(1710)$, can be described as quarkonium states. In this case we follow the view [41] that these f_0 states result from the mixing of two scalar-isoscalar $q\bar{q}$ states and an additional isosinglet glueball configuration predicted to reside in this mass regime. It should be noted that our

very sensitive to the detailed mixing scheme residing in this f_0 sector. Out of the three mesons $f_0(1370)$, $f_0(1500)$ and $f_0(1710)$ we may take any two and treat them in the meson exchange diagrams as if they were quarkonium states. Here, for simplicity, we take the two lowest scalars $f_0(1370)$ and $f_0(1500)$.

An estimate of the radiative decays of 3P_0 quarkonia states done in Refs. [22, 23] shows that the decay width $f_0 \rightarrow \rho^0 + \gamma$ is rather large with $\Gamma_{f_0 \rightarrow \rho\gamma} = 125$ KeV assuming a mass of $M_{f_0} = 0.98$ GeV. This means that the coupling constant should have the value $g_{\rho f_0 \gamma} = 1.3$, i.e. about five times larger than the value used in the calculations. Starting with this alternative estimate of the coupling constant we recalculated the cross sections σ_L and σ_T substituting for the cases of $f_0(1370)$ and $f_0(1500)$ the value $g_{\rho f_0 \gamma} = 1.3$ instead of $g_{\rho f_0 \gamma} = 0.25$. Here we suppose that the true quarkonia states lie above $\sim 1.2 - 1.3$ GeV (and thus $f_0(980)$ is not a 3P_0 quarkonium state), but the behavior of the quarkonia wave function at the origin $R_{q\bar{q}}(r \rightarrow 0)$ (which defines the value of $g_{\rho f_0 \gamma}$) does not change significantly if the mass of the $q\bar{q}$ system used in calculation of the $f_0 \rightarrow \rho_0 \gamma$ branching will increase from 0.98 GeV to 1.4 – 1.5 GeV.

In Fig. 6 we present the results of this recalculation (the notations are the same as in Fig. 5). The influence of the change of couplings on σ_T is negligible consistent with a relatively small contribution of f_0 exchanges to σ_T . At the same time the longitudinal cross section σ_L is increased considerably and now theoretical curves shown in Fig. 6 are in good agreement with the data [1] within experimental errors.

Recall that the CLAS data at $x_B = 0.31$ and 0.38 correspond to invariant energies W mostly above the resonance region ($W \cong 2 - 2.2$ GeV). At lower energies (i.e. at $x_B = 0.45$ and 0.52 in the CLAS data) theoretical predictions failed to explain the data (Fig. 7). It is possible that the enhancements of the cross sections observed in the region $W \cong 1.95 - 2$ GeV (this region corresponds to $Q^2 \cong 2.4 - 2.6$ GeV $^2/c^2$ at fixed $x_B = 0.45$ in Fig. 7) are consistent with some high-mass baryon resonances. A similar enhancement is also seen in σ_T at $x_B = 0.38$ near $Q^2 \cong 1.7 - 1.8$ GeV $^2/c^2$ (i.e. near $W \approx 1.95$ GeV), but unfortunately the experimental uncertainties (especially for σ_L) are too large in this region. It is interesting to note that our theoretical curves represented in Fig. 7 for all the kinematical region of the CLAS experiment are well correlated (with only one exception for σ_L at $x_B = 0.31$) with the theoretical curves of Ref. [1] obtained on the basis of a Regge model [13–16].

The new published CLAS data at electron beam energy $E_e = 5.754$ GeV with full information on differential cross sections [2] allow a more detailed test of our results. In the region of quasi-elastic knockout $|t - t_{min}| \lesssim (0.2 - 0.3)$ GeV $^2/c^2$ these results can be considered as predictions and can be used in the analysis of differential cross sections. In Fig. 8 we show the results for $d\sigma_T(t, W, Q^2)/dt$ and $d\sigma_L(t, W, Q^2)/dt$ calculated in the kinematics above

2.2 GeV²/c²) using enhanced values for $g_{\rho f_0 \gamma}$ as done for the satisfactory description of $\sigma_{L,T}$ (Figs. 6 – 7). The transverse cross section $d\sigma_T/dt$ largely depends on the sign of the interference term between pseudoscalar- and pseudovector-meson exchange contributions (the last column of Table IV), and thus we show in Fig. 8 two cases: destructive (solid lines) and constructive (dashed lines) interference of the S_5 and V_5 contributions. As can be seen from Fig. 8 the variant with destructive interference correlates well with the CLAS data on both $d\sigma_L/dt$ and $d\sigma_T/dt$ at small $|t|$ close to the quasi-elastic knockout region. For larger values of $|t| \gtrsim 1$ GeV our prediction underestimates the data, but this deviation may not greatly change the integrated cross sections $\sigma_{L/T}$. For this reason, our model predictions, originally fitted to the old CLAS data on the integrated cross sections $\sigma_{L/T}$, also succeed in a satisfactory description of the new data on $d\sigma_{L/T}/dt$ [2].

The full analysis of the new CLAS data [2] will be presented in its own right in a separate forthcoming paper. The analysis of this new high-precision experimental information in terms of the above model could clarify the role of scalar mesons in the ρ^0 electroproduction and, finally, could give definite constraints on the free parameters of the effective Lagrangians: coupling constants and form factors.

We also should comment on the possible role of the “non-correlated” two-pion exchange mechanism not considered here. The explicit contribution of the three-pion box diagram to the ρ^0 photoproduction was studied in Ref. [10] (note that the meson exchange parameters used in Ref. [10] are practically the same as in the present model). The calculations performed for values of $E_\gamma = 2.8, 3.28, 3.55$ and 3.82 GeV shown that the contribution of this mechanism to the differential cross section becomes comparable to other contributions only for the very forward and backward angles, e.g. for $|t| \lesssim 0.1 - 0.2$ GeV²/c². Recall that the threshold value of $t = t_{min}^0$ for the ρ photoproduction is very small ($|t_{min}^0| \approx 0$) when compared to the electroproduction threshold value t_{min}^Q at $Q^2 \gtrsim 1.5 - 2$ GeV²/c² (e.g., values of $|t_{min}^Q| \gtrsim 0.2 - 0.4$ GeV²/c² are characteristic of the CLAS kinematics as can be seen from Fig. 8). Based on the results of Ref. [10] we therefore think that the non-correlated two-pion exchange does not significantly change our results at $|t| \gtrsim 0.2 - 0.4$ obtained for the CLAS kinematics with $|t_{min}^Q| \gtrsim 0.2 - 0.4$ GeV²/c². But we also plan to perform an exact evaluation of the 2π contribution to $d\sigma_{L,T}/dt$ in a full analysis of the new CLAS data.

Acknowledgments

This work was supported by the DFG under Contract No. FA67/31-2 and No. GRK683. The work is par-

tially supported by the DFG under Contract No. 436 RUS 113/988/01 and by the grant No. 09-02-91344 of RFBR (the Russian Foundation for Basic Research). This research is also part of the European Community-Research Infrastructure Integrating Activity “Study of Strongly Interacting Matter” (HadronPhysics2, Grant Agreement No. 227431) and of the President grant of Russia “Scientific Schools” No. 871.2008.2. The work is partially supported by Russian Science and Innovations Federal Agency under contract No 02.740.11.0238.

Appendix A: Coefficients A_T, B_T, C_T, D_T

The coefficients A, B, C, D and E in Eqs.(52) and (54) are polynomials in Q, t and W . In particular, the coefficients A_T, B_T, C_T and D_T which are rather lengthy and not shown in Table III can be written in the form:

$$\begin{aligned} A_T &= \sum_{n=-2}^4 \left(\frac{Q}{m_N} \right)^n a_n(\eta, \xi_s, \xi_t), \\ B_T &= \sum_{n=-2}^4 \left(\frac{Q}{m_N} \right)^n b_n(\eta, \xi_s, \xi_t), \dots, \end{aligned} \quad (\text{A1})$$

where the coefficients a_n, b_n, \dots are polynomials in three dimensionless variables:

$$\begin{aligned} \eta &= \frac{-t}{4m_N^2}, \quad \xi_s = \frac{pq}{m_N Q} = \frac{Q}{2m_N x_B}, \\ \xi_t &= \frac{kq}{m_N Q} = \frac{Q}{2m_N} + \frac{M_\rho^2 - t}{2m_N Q}. \end{aligned} \quad (\text{A2})$$

Here we use the standard designation for Bjorken’s variable $x_B = \frac{Q^2}{2pq}$ and introduce relative values $\mu_\rho = \frac{m_N}{M_\rho}$ and $\mu_f = \frac{m_N}{M_f}$ to simplify formulas. In terms of these variables the polynomials a_n, b_n, c_n and d_n for $n = -2, -1, \dots, 4$ take the form:

$$\begin{aligned} a_{-2} &= -\frac{64}{9} \eta^2 (\eta + 1) (4\eta \mu_f^2 + 1)^2, \\ b_{-2} &= \frac{64}{9} \mu_\rho^2 \eta^2 (\eta + 1) (4\eta \mu_f^2 + 1)^2, \\ c_{-2} &= 0, \\ d_{-2} &= 0; \end{aligned} \quad (\text{A3})$$

$$\begin{aligned}
a_{-1} &= \frac{256}{9}\eta(8\eta^2(\eta+1)\mu_f^4 + 6\eta(\eta+1)\mu_f^2 + \eta+1)\xi_t, \\
b_{-1} &= -\frac{32}{9}\xi_t\eta(4\eta\mu_f^2 + 1)\{4[8\eta(\eta+1)\mu_\rho^2 + \eta+1]\mu_f^2 + 8(\eta+1)\mu_\rho^2 - 3\}, \\
c_{-1} &= \frac{128}{3}\eta(4\eta\mu_f^2 + 1)\xi_t, \\
d_{-1} &= -\frac{64}{3}\eta(4\eta\mu_f^2 + 1)\xi_t;
\end{aligned} \tag{A4}$$

$$\begin{aligned}
a_0 &= -\frac{512}{3}\mu_f^4\xi_t^2\eta^2(\eta+1) - \frac{128}{9}\mu_f^2\eta[-12\eta\xi_s(\xi_s - \xi_t) + \xi_t^2(6\eta+9) + 8\eta(\eta+1)] \\
&\quad - \frac{16}{9}(-24\eta\xi_s(\xi_s - \xi_t) + \xi_t^2(16 + \eta - 9\eta^2) + 16\eta(\eta+1)), \\
b_0 &= \frac{256}{9}\mu_f^4\eta(\eta+1)[4\eta(5\xi_t^2 + 2\eta)\mu_\rho^2 + 3\xi_t^2 + 2\eta] \\
&\quad + \frac{128}{9}\mu_f^2\{-2\eta^2 - \xi_t^2\eta + 6\mu_\rho^2\eta[-2\eta\xi_s^2 + 3\eta\xi_t\xi_s + (2\eta+3)\xi_t^2 + 2\eta(\eta+1)] + \eta + 2\xi_t^2\} \\
&\quad + \frac{4}{9}\{9\eta\xi_t^2 - 75\xi_t^2 - 24\eta + 4\mu_\rho^2[-24\eta\xi_s^2 + 36\eta\xi_t\xi_s + (-9\eta^2 + 4\eta + 16)\xi_t^2 + 16\eta(\eta+1)]\}, \\
c_0 &= -\frac{64}{3}(8\eta(\xi_t^2 + \eta)\mu_f^2 + (3\eta^2\mu_\rho^2 + 7)\xi_t^2 + 2\eta), \\
d_0 &= \frac{128}{3}\mu_f^2\eta[-\mu_\rho^2\eta\xi_t(2\xi_s - \xi_t) + 2(\xi_t^2 + \eta)] + \frac{32}{3}[7\xi_t^2 + 2\eta + \eta\mu_\rho^2\xi_t(-2\xi_s + 3\eta\xi_t + \xi_t)];
\end{aligned} \tag{A5}$$

$$\begin{aligned}
a_1 &= \frac{512}{9}\mu_f^4\xi_t^3\eta(\eta+1) + \frac{128}{9}\mu_f^2\xi_t[-12\eta\xi_s^2 + 12\eta\xi_t\xi_s - (\eta-2)\xi_t^2 + 8\eta(\eta+1)] \\
&\quad + \frac{32}{9}\xi_t[-6\xi_t^2 - 24\xi_s(\xi_s - \xi_t) + (\eta+1)(16 - 9\eta)], \\
b_1 &= -\frac{128}{9}\mu_f^4\xi_t[4\mu_\rho^2\eta(\eta+1)(4\xi_t^2 + 9\eta) + (\eta+1)(\xi_t^2 + 8\eta)] \\
&\quad - \frac{64}{9}\mu_f^2\{2\mu_\rho^2[6\eta\xi_s(6\xi_t^2 + \eta) - 24\eta\xi_s^2\xi_t + (4 - 8\eta)\xi_t^3 + \eta(22\eta + 25)\xi_t] + \xi_t(-6\xi_s^2 + 6\xi_t\xi_s - 3\xi_t^2 + 2\eta + 8)\} \\
&\quad - \frac{8}{9}\mu_\rho^2\{\xi_t[-36\eta^2 - 3(3\eta + 16)\xi_t^2 + 52\eta + 64 - 96\xi_s^2] + 24\xi_s(6\xi_t^2 + \eta)\} - \frac{8}{3}\xi_t(12\xi_s^2 + 3\eta - 6\xi_s\xi_t - 25), \\
c_1 &= \frac{128}{3}\mu_f^2\xi_t(\xi_t^2 + 4\eta) + 32\mu_\rho^2\xi_t(\xi_t^2 + 4\eta) + \frac{32}{3}\xi_t(-12\xi_s^2 - 3\xi_t^2 + 12\xi_s\xi_t + 28), \\
d_1 &= \frac{128}{3}\mu_f^2\mu_\rho^2(2\xi_s - \xi_t)\eta(2\xi_t^2 + \eta) - \frac{16}{3}\mu_\rho^2\xi_t[(3\eta + 4)\xi_t^2 + 2\eta(6\eta + 1)] + \frac{64}{3}\mu_\rho^2\xi_s(2\xi_t^2 + \eta) \\
&\quad - \frac{8}{3}\xi_t[8(\xi_t^2 + 4\eta)\mu_\rho^2 - 24\xi_t^2 - 3\xi_t^2 + 18\xi_t\xi_s + 56].
\end{aligned} \tag{A6}$$

$$\begin{aligned}
a_2 &= -\frac{64}{9}\mu_f^4\xi_t^4(\eta+1) + \frac{32}{9}\mu_f^2\xi_t^2\{3[\xi_t^2+4\xi_s(\xi_s-\xi_t)]-8(\eta+1)\}-4\mu_\rho^2\eta\xi_t^2[\xi_t^2+4\xi_s(\xi_s-\xi_t)] \\
&\quad -\frac{16}{3}(2\xi_s-\xi_t)^2[3\xi_s(\xi_s-\xi_t)+3\eta-4]-\frac{4}{9}(-36\eta^2+28\eta+64), \\
b_2 &= \frac{128}{9}\mu_f^4(\eta+1)[2\mu_\rho^2(\xi_t^4+8\eta\xi_t^2+4\eta^2)+\xi_t^2+2\eta] \\
&\quad +\frac{64}{9}\mu_f^2\{2\mu_\rho^2[-3(2\xi_s^2-\xi_t^2)(\xi_t^2+2\eta)+8\eta(\eta+1)+\xi_s(9\xi_t^3+30\eta\xi_t)]-6\xi_s^2-3\xi_t^2+4\eta+6\xi_s\xi_t+4\} \\
&\quad +\frac{4}{3}\mu_\rho^2\xi_s^2(48\xi_s^2-144\xi_s\xi_t+129\xi_t^2+48\eta-64) \\
&\quad +\frac{4}{9}\mu_\rho^2\{-12\xi_s\xi_t(9\xi_t^2+18\eta-32)+4[-9\eta^2+9(\eta-4)\xi_t^2+16(\eta+1)]\}+\frac{4}{3}(24\xi_s^2+3\eta-12\xi_s\xi_t-25), \\
c_2 &= -\frac{128}{3}\mu_f^2\xi_t^2-\frac{4}{3}\mu_\rho^2[-9\xi_t^4+48\xi_s\xi_t^3+48(\eta-\xi_s^2)\xi_t^2+48\eta^2]-\frac{32}{3}(-12\xi_s^2+12\xi_t\xi_s-3\xi_t^2+14), \\
d_2 &= -\frac{64}{3}\mu_f^2\mu_\rho^2\xi_t[-\xi_t^3+2\xi_s(\xi_t^2+6\eta)-6\eta\xi_t]+\frac{64}{3}\mu_f^2\xi_t^2+\frac{4}{3}(-48\xi_s^2-6\xi_t^2+36\xi_s\xi_t+56) \\
&\quad +\frac{4}{3}\mu_\rho^2[48\xi_t\xi_s^3-96\xi_t^2\xi_s^2+\xi_t\xi_s(51\xi_t^2+24\eta-64)-6\xi_t^4+4(3\eta+8)\xi_t^2+24\eta^2]; \tag{A7}
\end{aligned}$$

$$\begin{aligned}
a_3 &= 8\eta\mu_\rho^2\xi_t(\xi_t-2\xi_s)^2, \\
b_3 &= -\frac{256}{9}\mu_f^4\mu_\rho^2(\eta+1)\xi_t(\xi_t^2+2\eta)-\frac{64}{3}\mu_f^2\mu_\rho^2\xi_s(-2\xi_s\xi_t+5\xi_t^2+4\eta)+\frac{128}{9}\mu_f^2\mu_\rho^2\xi_t(3\xi_t^2+\eta-2) \\
&\quad -\frac{24}{9}\mu_\rho^2\xi_s(-24\xi_s^2+39\xi_t\xi_s-15\xi_t^2-12\eta+16)-\frac{8}{9}\mu_\rho^2\xi_t(9\eta-24), \\
c_3 &= 8\mu_\rho^2\xi_t(-16\xi_s^2+16\xi_t\xi_s-3\xi_t^2+4\eta), \\
d_3 &= \frac{32}{3}\mu_f^2\mu_\rho^2(2\xi_s-\xi_t)(3\xi_t^2+4\eta)-\frac{32}{3}\mu_\rho^2\xi_s(6\xi_s^2-15\xi_t\xi_s-9\xi_t^2-3\eta+4)-\frac{4}{3}\mu_\rho^2\xi_t(-9\xi_t^2+16); \tag{A8}
\end{aligned}$$

$$\begin{aligned}
a_4 &= -4\eta\mu_\rho^2(\xi_t-2\xi_s)^2, \\
b_4 &= \frac{64}{9}\mu_f^4\mu_\rho^2\xi_t^2(1+\eta)+\frac{32}{3}\mu_f^2\mu_\rho^2\xi_t(2\xi_s-\xi_t)+4\mu_\rho^2\xi_s(3\xi_s-2\xi_t), \\
c_4 &= 4\mu_\rho^2(16\xi_s^2-16\xi_t\xi_s+3\xi_t^2), \\
d_4 &= -\frac{32}{3}\mu_f^2\mu_\rho^2\xi_t(2\xi_s-\xi_t)-4\mu_\rho^2(8\xi_s^2-7\xi_t\xi_s+\xi_t^2). \tag{A9}
\end{aligned}$$

-
- [1] C. Hadjidakis *et al.* (CLAS Collaboration), Phys. Lett. B **605**, 256 (2005).
[2] S. A. Morrow *et al.* (CLAS Collaboration), Eur. Phys. J. A **39**, 5 (2009).
[3] M. Battaglieri *et al.* (CLAS Collaboration), Phys. Rev. Lett. **87**, 172002 (2001); M. Battaglieri *et al.* (CLAS Collaboration), Phys. Rev. Lett. **90**, 022002 (2003).
[4] G. M. Huber *et al.* (Jefferson Lab. F_π Collab.), Phys. Rev. C **78**, 045203 (2008).
[5] T. Horn *et al.* (Jefferson Lab. F_π Collab.), Phys. Rev. Lett. **97**, 192001 (2006).
[6] J. Volmer *et al.* (Jefferson Lab. F_π Collab.), Phys. Rev. Lett. **86**, 1713 (2001).
[7] A. Faessler, T. Gutsche, V. E. Lyubovitskij and I. T. Obukhovskiy, Phys. Rev. C **76**, 025213 (2007).
[8] D. G. Cassel *et al.* Phys. Rev. D **24**, 2787 (1981).
[9] B. Renner, Nucl. Phys. B **30**, 634 (1971); B. Renner, Phys. Lett. B **33**, 599 (1970).
[10] Y. S. Oh and T. S. H. Lee, Phys. Rev. C **69**, 025201 (2004).
[11] M. Guidal and S. Morrow, *Proceedings of the International Workshop Exclusive reactions at high momentum transfer, Jefferson Laboratory, Newport-News, Virginia, USA, May 21-24 2007* (World Scientific, 2008) ISBN 9812796940, arXiv:0711.3743 [hep-ph].
[12] M. M. Kaskulov, K. Gallmeister and U. Mosel, Phys. Rev. D **78**, 114022 (2008); M. M. Kaskulov and U. Mosel, Phys. Rev. C **80**, 028202 (2009).
[13] J. M. Laget and R. Mendez-Galain, Nucl. Phys. A **581**, 397 (1995).
[14] M. Guidal, J. M. Laget and M. Vanderhaeghen, Nucl. Phys. A **627**, 645 (1997).

- [15] J. M. Laget, Phys. Rev. D **70**, 054023 (2004); J. M. Laget, Phys. Lett. B **489**, 313 (2000); J. M. Laget, Nucl. Phys. A **699**, 184c (2002).
- [16] F. Cano and J. M. Laget, Phys. Lett. B **551**, 317 (2003) [Erratum-ibid. B **571**, 250 (2003)].
- [17] A. Donnachie and P. V. Landshoff, Nucl. Phys. B **244**, 322 (1984); A. Donnachie and P. V. Landshoff, arXiv:0803.0686 [hep-ph].
- [18] I. T. Obukhovskiy, D. Fedorov, A. Faessler, T. Gutsche and V. E. Lyubovitskij, Phys. Lett. B **634**, 220 (2006).
- [19] V. G. Neudatchin, I. T. Obukhovskiy, L. L. Sviridova and N. P. Yudin, Nucl. Phys. A **739**, 124 (2004).
- [20] M. N. Achasov *et al.* (SND Collab.), Phys. Lett. B **537**, 201 (2002).
- [21] C. Amsler *et al.* [Particle Data Group], Phys. Lett. B **667**, 1 (2008).
- [22] Yu. Kalashnikova, A. E. Kudryavtsev, A. V. Nefediev, J. Haidenbauer and C. Hanhart, Phys. Rev. C **73**, 045203 (2006).
- [23] F. E. Close, A. Donnachie and Yu. S. Kalashnikova, Phys. Rev. D **67**, 074031 (2003).
- [24] B. Friman and M. Soyeur, Nucl. Phys. A **600**, 477 (1996).
- [25] L. S. Kisslinger, Nucl. Phys. A **629**, 30c (1998); L. S. Kisslinger and W. H. Ma, Phys. Lett. B **485**, 367 (2000); L. S. Kisslinger and M. B. Johnson, Phys. Lett. B **523**, 127 (2001).
- [26] G. V. Efimov and M. A. Ivanov, *The Quark Confinement Model of Hadrons*, (IOP Publishing, Bristol & Philadelphia, 1993).
- [27] M. A. Ivanov, M. P. Locher and V. E. Lyubovitskij, Few Body Syst. **21**, 131 (1996); M. A. Ivanov, V. E. Lyubovitskij, J. G. Körner and P. Kroll, Phys. Rev. D **56**, 348 (1997) [arXiv:hep-ph/9612463].
- [28] A. Faessler, T. Gutsche, M. A. Ivanov, V. E. Lyubovitskij and P. Wang, Phys. Rev. D **68**, 014011 (2003).
- [29] T. Branz, T. Gutsche and V. E. Lyubovitskij, Eur. Phys. J. A **37**, 303 (2008).
- [30] M. Kirchbach and L. Tiator, Nucl. Phys. A **604**, 385 (1996).
- [31] A. I. Titov, T. S. Lee, H. Toki and O. Streltsova, Phys. Rev. C **60**, 035205 (1999).
- [32] T. Hatsuda, Nucl. Phys. B **329**, 376 (1990).
- [33] R. N. Cahn, Phys. Rev. D **35**, 3342 (1987).
- [34] F. E. Close, A. Donnachie and Yu. S. Kalashnikova, Phys. Rev. D **65**, 092003 (2002).
- [35] T. Bolton *et al.*, Phys. Lett. B **278**, 495 (1992).
- [36] M. Kirchbach and D. O. Riska, Nucl. Phys. A **594**, 419 (1995); M. Kirchbach, L. Tiator, S. Neumeier and S. Kamalov, arXiv:nucl-th/9609021.
- [37] J. R. Ellis and M. Karliner, Phys. Lett. B **313**, 131 (1993).
- [38] J. P. Santoro *et al.* (CLAS Collaboration), Phys. Rev. C **78**, 025210 (2008).
- [39] E. van Beveren, T. A. Rijken, K. Metzger, C. Dullemond, G. Rupp and J. E. Ribeiro, Z. Phys. C **30**, 615 (1986); E. van Beveren and G. Rupp, Eur. Phys. J. A **31**, 468 (2007).
- [40] N. A. Tornqvist and M. Roos, Phys. Rev. Lett. **76**, 1575 (1996).
- [41] F. Giacosa, T. Gutsche, V. E. Lyubovitskij and A. Faessler, Phys. Rev. D **72**, 094006 (2005).
- [42] Y. Chen *et al.*, Phys. Rev. D **73**, 014516 (2006); J. Sexton, A. Vaccarino and D. Weingarten, Nucl. Phys. Proc. Suppl. **47**, 128 (1996).

Table I. $SU(3)_F \times O(3)$ classification of neutral mesons contributing to the electroproduction of ρ^0 (the octet-singlet mixing is omitted for simplicity). Quark model (QM) and hadronic molecular (HM) states usually used for description of meson properties are also shown (including a possible scalar glueball G_0).

$I^G(J^{PC})$	QM ($^{2S+1}L_J$) or HM	$SU(3)$ octet states	$SU(3)$ singlet states
$0^+(0^{-+})$	1S_0	$\eta(540)$	$\eta'(958)$
$1^-(0^{-+})$	1S_0	$\pi(140)$	
$0^+(0^{++})$	$K\bar{K}, 2\pi$	$f_0(980)$	$f_0(600) \equiv \sigma$
$0^+(0^{++})$	3P_0	$f_0(1370)$	$f_0(1500)$
$0^+(0^{++})$	(G_0)		$f_0(1710)$
$0^+(1^{++})$	3P_1	$f_1(1285)$	$f'_1(1420)$
$0^+(2^{++})$	3P_2	$f_2(1270)$	$f'_2(1525)$
$1^-(0^{++})$	$K\bar{K}$	$a_0(980)$	
$1^-(0^{++})$	3P_0	$a_0(1450)$	
$1^-(1^{++})$	3P_1	$a_1(1260)$	
$1^-(2^{++})$	3P_2	$a_2(1320)$	

Table II. Expressions for the $\rho M \gamma$ and MNN vertices

M	$S_5(\eta, \pi^0)$	$V_5(f_1, a_1)$	$S(f_0, a_0)$	$T(f_2, a_2)$
$\Gamma_M^{\nu, \mu\nu}$	$-eg_{\rho M \gamma} \varepsilon^{\mu\nu\alpha\beta} \frac{q_\alpha k'_\beta}{M_\rho}$	$-eg_{\rho M \gamma} \varepsilon^{\mu\nu\alpha\beta} \frac{k'^2 q_\beta - q^2 k'_\beta}{M_\rho^2}$	$eg_{\rho M \gamma} \frac{qk'}{M_\rho} \left(g^{\mu\nu} - \frac{q^\mu k'^\nu}{qk'} \right)$	$eg_{\rho M \gamma} \frac{1}{M_T} \left[g^{\mu\nu} (q+k')^\alpha (q+k')^\beta - g^{\mu\alpha} k'^\nu (q+k')^\beta - g^{\mu\beta} k'^\nu (q+k')^\alpha - g^{\nu\alpha} q^\mu (q+k')^\beta - g^{\nu\beta} q^\mu (q+k')^\alpha + 2qk' (g^{\nu\alpha} g^{\mu\beta} + g^{\nu\beta} g^{\mu\alpha}) \right]$
Γ_M^ν	$\frac{g_{MNN}}{2m_N} k \gamma^5$	$g_{MNN} \gamma^\alpha \gamma^5$	g_{MNN}	$\frac{g_{MNN}}{m_N} [(p+p')^\alpha \gamma^\beta + (p+p')^\beta \gamma^\alpha]$

Table III. Coefficients A_M, B_M, C_M, D_M and E_M of Eq. (52)

M	$S_5(\eta, \pi^0)$	$V_5(f_1, a_1)$	$S(f_0, a_0)$	$T(f_2, a_2)$
A_M	$-\eta(\xi_t^2 - 4\eta)$	$2 - \xi_s^2 + \xi_s \xi_t - (\xi_t^2 - 4\eta) \frac{m_N^2}{M_\rho^2} \left[\frac{m_N^2}{Q^2} (1 + \eta) + \frac{2M_\rho^2}{M_{V_5}^2} (1 + 2\eta \frac{m_N^2}{M_{V_5}^2}) \right] + z^2 (1 + \eta) \left[\frac{4m_N^2}{Q^2} \eta - (\xi_t^2 - 4\eta) \frac{m_N^2}{M_\rho^2} \right] + z \frac{2m_N}{Q} [2\eta \xi_s - (1 + 2\eta) \xi_t]$	$(1 + \eta) \left(\frac{M_\rho^2}{m_N^2} - \xi_t^2 + 4\eta \right)$	*
B_M	η	$\frac{m_N^2}{M_\rho^2} \left[\frac{m_N^2}{Q^2} (1 + \eta) + \frac{2M_\rho^2}{M_{V_5}^2} (1 + 2\eta \frac{m_N^2}{M_{V_5}^2}) \right] + z^2 \left[\frac{m_N^2}{Q^2} (1 + 2\eta) + \frac{m_N^2}{M_\rho^2} (1 + \eta) \right]$	$1 + \eta$	*
C_M	0	$1 + z^2 \frac{4m_N^2}{Q^2} \eta - z \frac{2m_N}{Q} \xi_t$	0	*
D_M	0	$-\frac{1}{2} - z^2 \frac{2m_N^2}{Q^2} \eta + z \frac{m_N}{Q} \xi_s$	0	*
E_M	0	$\frac{m_N^4}{M_\rho^2 Q^2} (1 + z^2)$	0	0
$\tilde{g}_{\rho M \gamma}$	$\frac{m_N}{M_\rho} g_{\rho S_5 \gamma}$	$\frac{Q^2}{z M_\rho^2} g_{\rho V_5 \gamma}, \quad z = \frac{Q^2}{M_\rho^2 + Q^2}$	$\frac{m_N}{M_\rho} g_{\rho S \gamma}$	$\frac{m_N}{M_T} g_{\rho T \gamma}$
\mathcal{N}_M	$\tilde{e} g_{\rho M \gamma} g_{MNN} \mathcal{F}_{\rho M \gamma}(Q^2, t) \mathcal{F}_{MNN}(t) 2m_N Q / (M_M^2 - t)$			

*) see A_T, B_T, C_T and D_T in Appendix

Table IV. $A_{MM'}$, $B_{MM'}$, $C_{MM'}$, $D_{MM'}$ and $E_{MM'}$ of Eq. (54)

MM'	ST	S_5V_5
$A_{MM'}$	$-8 \left(\frac{Q}{m_N} - \xi_t \right) \left\{ \frac{Q}{m_N} (2\xi_s - \xi_t)^2 - \frac{4}{3}(1+\eta) \left[2 \left(\frac{Q}{m_N} - \xi_t \right) + \eta \frac{m_N}{Q} + \frac{m_N^2}{M_T^2} \frac{Q}{m_N} \left(\xi_t - 2\eta \frac{m_N}{Q} \right)^2 \right] \right\}$	$-(\xi_t^2 - 4\eta) \left(1 + \frac{4m_N^2}{M_{V_5}^2} \eta \right)$
$B_{MM'}$	$-8 \left(\frac{Q}{m_N} - \xi_t \right) \left[\xi_s - 2\frac{Q}{m_N} + \frac{4}{3}(1+\eta) \frac{m_N^2}{M_T^2} \right]$	$1 + \frac{4m_N^2}{M_{V_5}^2} \eta$
$C_{MM'}$	$32 \left(\frac{Q}{m_N} - \xi_t \right)^2$	0
$D_{MM'}$	$8 \left(\frac{Q}{m_N} - \xi_t \right) \left[2\xi_s + \xi_t - 2\frac{Q}{m_N} \right]$	0
$E_{MM'}$	0	0

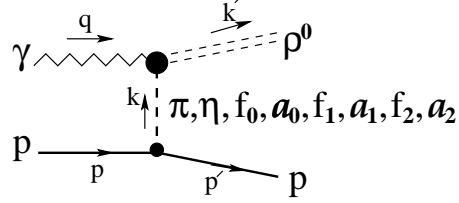


FIG. 1: t -pole amplitude generated by meson exchanges.

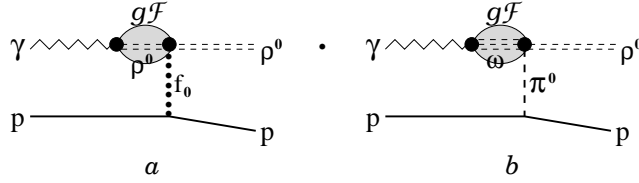


FIG. 2: Microscopic mechanism for the $\rho f_0 \gamma$ and $\rho \pi \gamma$ couplings.

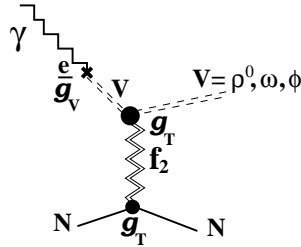


FIG. 3: Tensor meson contribution to the vector meson electroproduction in VMD and TMD models.

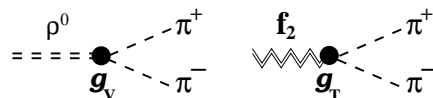


FIG. 4: Amplitudes of tensor meson decay into $\pi\pi$ in VMD and TMD models.

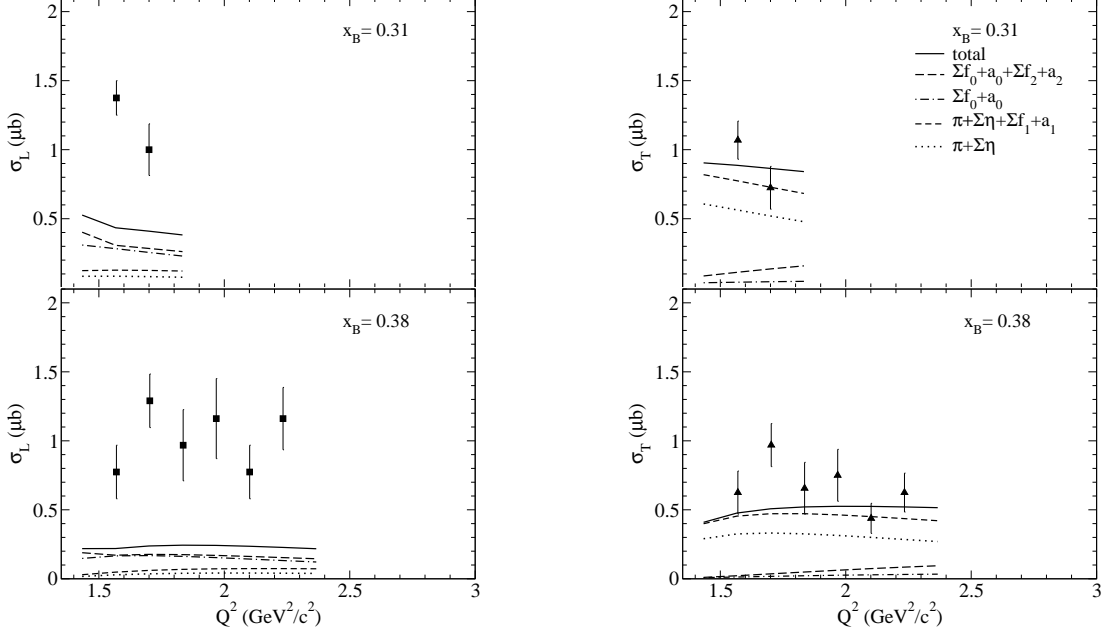


FIG. 5: Longitudinal (left panel) and transverse (right panel) cross sections σ_L and σ_T of ρ^0 electroproduction as functions of Q^2 . The sum of exchange contributions of all mesons listed in Table 1 is shown by solid lines. The sum of scalar meson contributions (dashed-dotted lines) is calculated with a common value of $g_{\rho f_0 \gamma} = 0.25$. The sum of contributions of scalar and tensor mesons is shown by long-dashed lines. The sum of pseudoscalar and pseudovector meson contributions is shown by short-dashed lines (the dotted lines show the pseudoscalar meson contributions). Experimental values are the recent CLAS data [1].

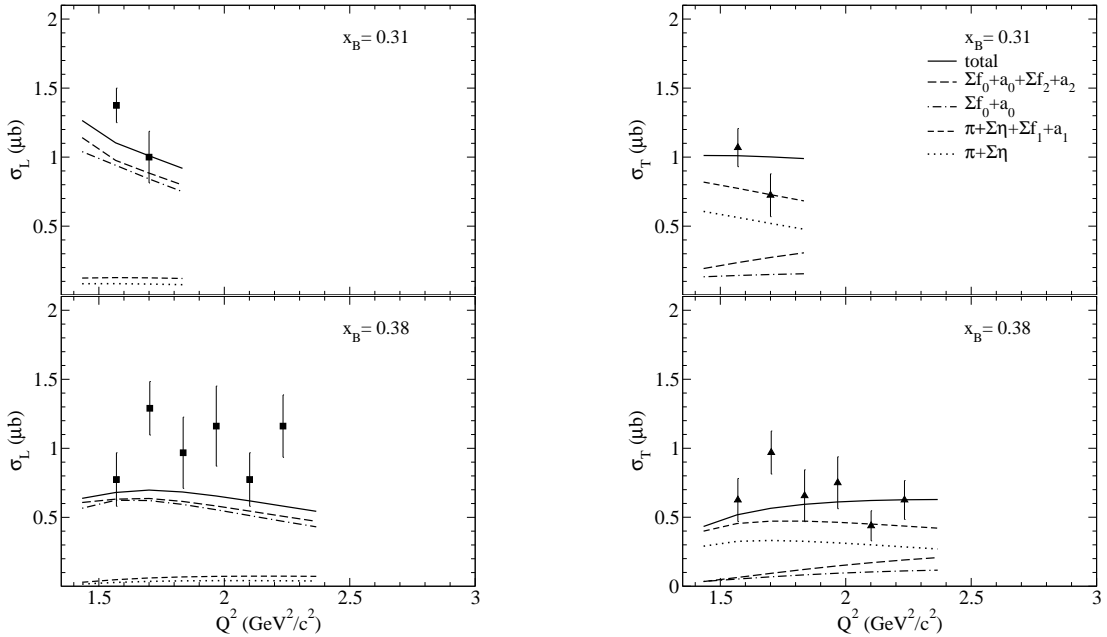


FIG. 6: The same results as in Fig. 5 but with an enhanced $\rho f_0 \gamma$ coupling ($g_{\rho f_0 \gamma} = 1.3$) for the two scalar mesons $f_0(1370)$ and $f_0(1500)$ (and for $a_0(1450)$ we use the common rule (41): $g_{\rho a_0 \gamma} = \frac{1}{3} g_{\rho f_0 \gamma}$).

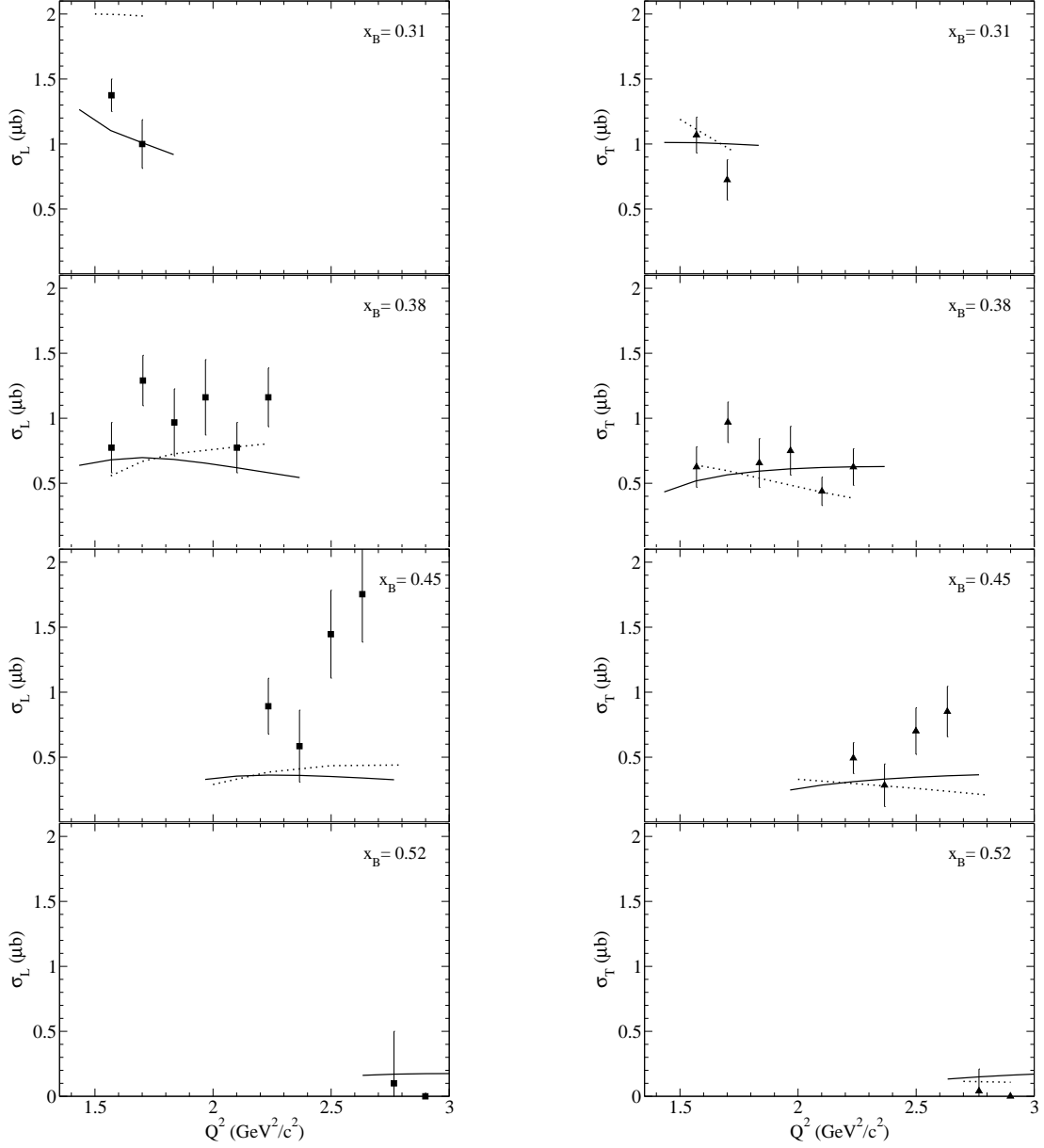


FIG. 7: Longitudinal (left panel) and transverse (right panel) cross sections of ρ^0 electroproduction. The last CLAS data [1] for $x_B = 0.31, 0.38, 0.45$ and 0.52 are shown in comparison to the theoretical curves. Solid lines correspond to the quasielastic knockout mechanism in which we take into account the full sum of exchange diagrams for intermediate mesons listed in Table 1. The results [1] obtained on the basis of a Regge model of Refs. [13–16] are also shown for comparison (dotted lines).

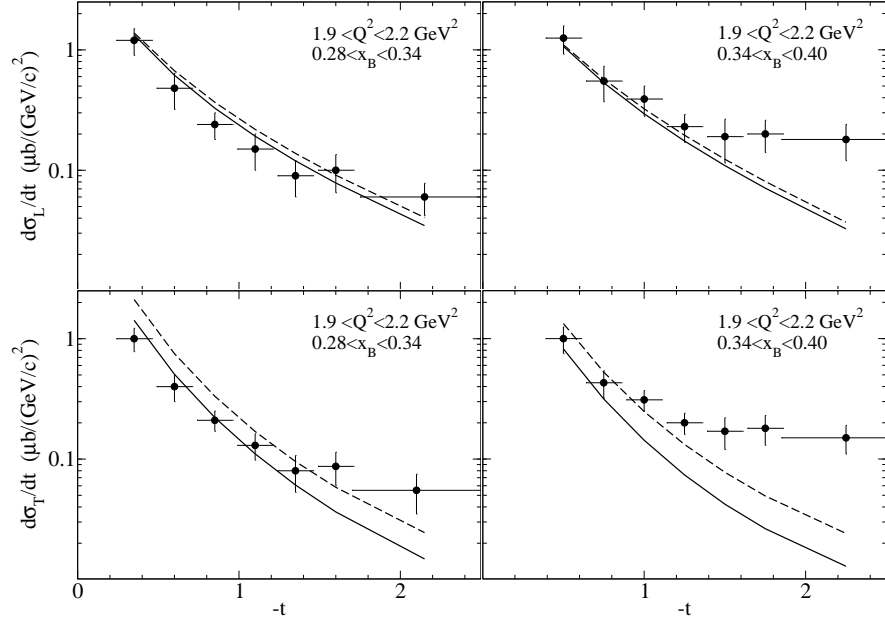


FIG. 8: Differential cross sections $d\sigma_L/dt$ (top panel) and $d\sigma_T/dt$ (bottom panel) averaged over intervals $0.28 < x_B < 0.34$ (left) and $0.34 < x_B < 0.40$ (right) at $1.9 < Q^2 < 2.2 \text{ GeV}^2/c^2$ calculated for the same values of $g_{\rho f_0 \gamma}$ as used in Figs. 6 and 7. Comparison with the latest CLAS data [2] for the respective experimental bins: the solid and dashed lines represent the results of calculations for the cases of destructive and constructive interference between contributions of pseudoscalar (S_5) and pseudovector (V_5) mesons respectively (the destructive interference corresponds to the inverse sign of expressions in the last column of Table IV).